Applied Soft Computing 61 (2017) 622–641

Contents lists available at ScienceDirect

Applied Soft Computing

journal homepage: www.elsevier.com/locate/asoc

Modified differential evolution algorithm for contrast and brightness enhancement of satellite images

Shilpa Suresh, Shyam Lal*

Department of Electronics & Communication Engineering, National Institute of Technology Karnataka, Surathkal, Mangaluru 575025, India

ARTICLE INFO

Article history:
Received 10 February 2017
Received in revised form 5 July 2017
Accepted 7 August 2017
Available online 17 August 2017

Keywords:
Image enhancement
Metaheuristics
Differential evolution algorithm
Cuckoo search algorithm
Satellite images

ABSTRACT

Satellite images normally possess relatively narrow brightness value ranges necessitating the requirement for contrast stretching, preserving the relevant details before further image analysis. Image enhancement algorithms focus on improving the human image perception. More specifically, contrast and brightness enhancement is considered as a key processing step prior to any further image analysis like segmentation, feature extraction, etc. Metaheuristic optimization algorithms are used effectively for the past few decades, for solving such complex image processing problems. In this paper, a modified differential Modified Differential Evolution (MDE) algorithm for contrast and brightness enhancement of satellite images is proposed. The proposed algorithm is developed with exploration phase by differential evolution algorithm and exploitation phase by cuckoo search algorithm. The proposed algorithm is used to maximize a defined fitness function so as to enhance the entropy, standard deviation and edge details of an image by adjusting a set of parameters to remodel a global transformation function subjective to each of the image being processed. The performance of the proposed algorithm is compared with ten recent state-of-the-art enhancement algorithms. Experimental results demonstrate the efficiency and robustness of the proposed algorithm in enhancing satellite images and natural scenes effectively. Objective evaluation of the compared methods was done using several full-reference and no-reference performance metrics. Qualitative and quantitative evaluation results proves that the proposed MDE algorithm outperforms others to a greater extend.

1. Introduction

Satellite images are important for various applications in different domains of remote sensing such as geographical information systems, meteorology, astrology, geosciences, agriculture, education, etc. The visual quality of many such recorded images are dropped down over the process of digital image acquisition due to factors such as noise interference, uneven illumination and even in *D*/*A* conversion process. Even raw satellite images generally possess relatively narrow range of brightness values. Thus, increasing demand on high quality images necessitates an image quality improvement procedure before image analysis. Hence, image enhancement is been adopted as an elementary step in all digital image processing and analysis applications to improve the interpretability or information perceived by humans. Image enhancement techniques are summarized into two major categories, viz., spatial domain techniques and frequency domain techniques [1]. Contrast enhancement is one among the most common and useful spatial enhancement techniques, which expands the range of intensities in an image, facilitating subsequent tasks like object identification and detection.

One of the most simplest and common way for contrast enhancement is a global intensity transformation procedure utilizing look up tables or transformation functions to map the intensity values of the input image to a new set of values with improved parameters. For multi-band input images, the intensity transformation procedure should also assure an efficient color reproduction preserving the naturalness of the image.

Histogram Equalization (HE) is one among the basic methods adopted for global image enhancement which have its applications in different research areas, which include object tracking, medical image processing, etc. [1,2]. But HE based methods fail to maintain the average brightness level of the image, which may result in over or under-saturation of selected areas. Several improved versions including Bi-Histogram Equalization (BHE) [3], dualistic sub-image

* Corresponding author.
E-mail addresses: shilparagesh89@gmail.com (S. Suresh), shyam.mtec@gmail.com (S. Lal).

http://dx.doi.org/10.1016/j.asoc.2017.08.019
1568-4946/

HE [4], Recursive Mean Separate HE (RMSHE) [5], etc. were devised [6]. However, they failed to provide the optimal contrast enhancement since the iterations converge to null processing.

Hence, the use of present contrast enhancement techniques particularly for satellite images makes them suffer from severe artifacts such as saturation errors, distortion of edge details and brightness drifting which need to be minimized. Every minor detail in a remotely sensed image represents substantial information concerning both intensity levels and spatial locations. Because of these reasons, an enhancement technique for such images, not only need to improve the contrast but also need to ensure minimum pixel distortion equally for low and high intensity regions of the image.

Most of the traditional enhancement approaches are highly dependent on the image to be processed and hence require manual human intervention. The automation of image enhancement process requires defining an evaluation criterion valid across a wide range of image datasets. A parameterized transformation function evaluated by a fitness criterion can be hence adopted for this process. Metaheuristic algorithms are largely exploited for different image processing applications during the last few decades. The potential of such algorithms in following a guided random search path proved to be very useful for solving complex contrast enhancement problems. The role of such metaheuristic optimization algorithms in image enhancement process is to maximize the fitness (objective) function to find the optimal combination of intensity transformation parameters. Hybridization of such algorithms integrating population based and trajectory based metaheuristics have also received great interest recently, which efficiently balances the diversification and intensification components to form a finer optimization scheme.

The rest of the paper is organized as follows. Section 2 gives a comprehensive study of the relevant papers in image enhancement domain, covering literature published since the last two decades, concentrating more on optimization based algorithms. Section 3 gives a detailed discussion about the problem formulation for image enhancement. The proposed algorithm for image enhancement is explained in Section 4. Section 5 includes the simulation results and discussions of various algorithms compared. Section 6 concludes the discussion by highlighting the advantages of the proposed algorithm, giving scope for future investigations.

2. Related works

Analyzing the literature for past one decade, reveals the use of several metaheuristic algorithms for image enhancement applications in different domains; Genetic Algorithm (GA) being one of the earliest in the course. Pal et al. were reported to be among the pioneers who have used GA for selecting an appropriate image enhancement operator automatically for contrast enhancement [7]. Then, Saitoh proposed the use of GA to measure the fitness of a candidate solution by assessing the intensity of spatial edges present in the image [8]. He also devised a transformation relation connecting the input and output gray levels, to convert an original gray scale image to its contrast enhanced version. He was able to produce reasonably good results compared with other traditional approaches at the expense of processing time. In the same year, Munteanu and Lazarescu used real-coded Genetic Algorithm with a subjective fitness function to evolve the contrast-stretching curve and was tested successfully on a dataset comprising satellite images [9]. The authors introduced a new crossover operator, called Gaussian Uniform Crossover (GUX) to perform better mixing of genetic materials in the course of evolution. But the method suffers from a major drawback that the fitness criterion was highly subjective to the image being processed.

Later in 2000, Munteanu and Rosa proposed an automated real-coded Genetic Algorithm based image enhancement technique [10]. The task of GA was to adapt the parameters of a novel extension to a local enhancement technique, similar to the process of statistical scaling. Thus, the image contrast and other details present in the image were enhanced following a predefined fitness criterion. Experimental results were furnished to prove the proposed method to outperform traditional point operations like Histogram Equalization (HE) and Linear Contrast Stretching (LCS). In 2007, Braik et al. introduced another automatic enhancement technique using Particle Swarm Optimization (PSO) algorithm considering the image enhancement process as a non linear optimization problem subject to a set of constraints [11]. The authors used PSO algorithm to enhance the details in the image by tuning a set of parameters by maximizing an objective function. The evaluation results preserved the edge details and were computationally less complex compared with GA based method.

Similar approaches were put forward by Gorai and Ghosh, in the subsequent years using PSO for parameter optimization of image enhancement problem [12,13]. The authors compared the experimental results of their proposed method on a standard gray level image dataset and proved to outperform GA based image enhancement algorithm.

Later in 2009, Dos et al. proposed three different evolution approaches based on chaotic sequence for image enhancement [14]. The chaotic function is used to help the proposed technique minimize premature convergence ensuring a fast convergence. The authors adopted the same objective function as in the previous cited paper for enhancement problem optimization [12]. The authors tested the algorithm only for two gray scale images and provided the comparison results with traditional differential evolution (DE) algorithm only. Hence, they failed to provide analytical and statistical studies emphasizing the robustness of the proposed method.

Most of the contrast enhancement methods suffer from a noticeable drawback that the mean intensity of the image is disturbed in cost of enhancement. Since the mean intensity of the image also contributes to the information present in the image, it is sensible to maintain its mean intensity in order to avoid unwanted artifacts. Kwok et al. devised a Multi objective Particle Swarm Optimization (MPSO) based technique for enhancing the contrast of gray scale images preserving its mean intensity [15]. The authors considered entropy maximization of the transformed image as one objective function and gamma correction for intensity preservation as the other. The proposed technique was tested on gray scale images with different intensities and distribution. It succeeded in achieving significant contrast enhancement especially for images with concentrated gray levels, but showed instances of discrepancies to ideal cases by attaining maximum entropy values for zero intensity difference.

Shanmugavadivu and Balasubramanian also contributed in formulating a new method for contrast enhancement preserving brightness by avoiding the abrupt mean shift occurring during the process of equalization [16]. The method relied on segmenting the original image histogram using Otsu's method to two sub-bands and equalizing both of them independently by a set of optimized weighing constraints obtained using PSO. The equalized sub-bands were merged to produce the final contrast enhanced version. The authors experimentally investigated and proved that the proposed technique to have an edge over the other state-of-the-art techniques in terms of entropy and Contrast Improvement Factor (CIF). The method was less stable and computationally complex compared with other contemporary algorithms.

Ye et al. also proposed an adaptive enhancement method combining cuckoo search (CS) and PSO particularly for low contrast images [17]. The authors used PSO-CS for estimating the param-

eters for formulating the intensity transformation function. The quality of enhanced image was determined by evaluating a entropy based fitness criterion. Although it produced improved results compared with other optimization algorithms included in their paper for comparison, the selection of fitness function which was solely based on the entropy of transformed image proved to be less appropriate. It also introduced over enhancement of certain regions when tested on gray scale satellite images. Bhandari et al. used beta DE algorithm for parameter optimization for modeling the transformation matrix [18]. It produced better quality metric values compared with other state-of-the-art algorithms, but it faced a major drawback of enhancing noisy elements present in the image. Further none of the above optimization algorithms were tested for multiband images to evaluate its robustness.

Hybridization of metaheuristics received interest since it helped in a wise combination of exploration and exploitation phase. Hoseini and Shayesteh proposed a hybrid combination of Ant Colony Optimization (ACO), GA and Simulated Annealing (SA) and Gogna and Tayal used GA/PSO/DE-SA for image enhancement [19,20]. Although the use of trajectory based algorithms like SA ensured intensified solution search in promising areas, it resulted in making the algorithm computationally very complex and was more prone to premature convergence. Mahapatra et al. proposed hybrid algorithm combining PSO along with Negative Selection Algorithm (NSA) and was tested on Matlab library images [21]. The method yielded more number of edge pixels by optimizing the defined fitness function as compared with HE, LCS and PSO based image enhancement techniques. The use of optimization algorithms for enhancing images in frequency doTMMn were also found in literature [22]. The results were promising in terms of quality metric values compared. Recently in 2016, Singh et al. presented a comprehensive analytical evaluation on the use of different nature inspired algorithms for contrast enhancement of satellite images [23].

Most of the image enhancement approaches discussed in this section results in unnecessary artifacts in one or the other way, especially for satellite image datasets. In order to avoid the ill-effects caused by these, a modified differential Modified Differential Evolution (MDE) algorithm based image enhancement algorithm is proposed in this paper. The proposed MDE algorithm is developed combining the exploration phase by differential evolution algorithm and exploitation phase by cuckoo search algorithm.

The major contributions of this research paper are summarized as follows:

- The proposed algorithm improved the convergence rate of differential evolution algorithm by effectively avoiding its premature convergence, ensuring the best possible approximation of the global solution attainable. The adoption of *Lévy* flight strategy of cuckoo search algorithm enhanced the local exploitation capability of the proposed algorithm.
- The proposed algorithm was found to be more stable, and it also helped in conserving the mean intensity of the image, bringing naturalness to the processed image.
- Quantitative and qualitative experimental studies were undertaken to demonstrate the robustness and efficiency of the proposed enhancement algorithm in comparison with other state-of-the-art techniques for different satellite and natural image datasets.

3. Problem formulation

A global intensity transformation in spatial domain helps in enhancing the visual contrast of an image. A transformation function or a look-up table mapping the intensity values of the original image to a new set of values are commonly utilized for improving such image attributes. Hence, the main objective of an image enhancement procedure is to define an efficient transformation function for intensity mapping. An automatic image enhancement procedure also requires a fitness criterion to quantify the quality of the enhanced image and to acquire the optimum parameters for enhancement. Further, detailed discussions on the related functions used, and the proposed optimization algorithm for image enhancement are presented in following subsection.

3.1. Transformation function

A transformation function generates new intensity values for each of the pixels in the original image of dimension $M \times N$, transforming the image to its visually enhanced version making its interpretation simpler. It can be mathematically represented as in Eq. (1)

$$e_{i,j} = T_f(o_{i,j}) \tag{1}$$

where $o_{i,j}$ indicates the intensity value of a pixel in the original image referred by its corresponding (i, j) coordinate values, where i ranges from 1 to M, and j ranges from 1 to N and T_f denotes the transformation function used for generating the corresponding enhanced image represented as $e_{i,j}$.

Most of the conventional image enhancement techniques in spatial domain follow either of the two procedures, namely, global intensity transformation and local intensity transformation. Histogram Equalization being one among the most primitive image enhancement approach follow the former procedure, wherein the entire image space is mapped to a new one, effectively enhancing its visual attributes [1,24]. Although the procedure seems to be very simple, it badly suffers from the limitations due to over enhancement causing blurring of edge details. Whereas, the later, does the mapping process by selectively extracting the local information content of the image, using a window of a predefined size. The local image enhancement procedure is continued throughout the entire image by sliding the same window throughout the entire image [25,26]. The local image enhancement procedure is thus quite expensive and time consuming compared with the global transformation procedure [27]. The transformation function used in our proposed algorithm includes both global and local information for producing an enhanced image. The enhanced image is represented as Eq. (2).

$$e_{i,j} = E^f_{i,j}\left(o_{i,j} - c \times m^l_{i,j}\right) + \left(m^l_{i,j}\right)^a \tag{2}$$

where $m^l_{i,j}$ represents the local mean of (i, j)th pixel of input image over a range defined by a window of dimension $w \times w$ as given in Eq. (3) and 'a, c' are the two related parameters.

$$m^l_{i,j} = \frac{1}{w \times w}\sum_{i=1}^{w}\sum_{j=1}^{w} o_{i,j} \tag{3}$$

$E^f_{i,j}$ denotes the enhancement function as given in Eq. (4)

$$E^f_{i,j} = \frac{k \times m^g}{\sigma^l_{i,j} + b} \tag{4}$$

where k, b are two related parameters, $\sigma^l_{i,j}$ denotes the local standard deviation of (i, j)th pixel of the input image over a range defined by a window of dimension $w \times w$ and m^g denotes the global mean. The global mean m^g is given by Eq. (5) and local standard deviation $\sigma^l_{i,j}$ is given by Eq. (6)

$$m^g_{i,j} = \frac{1}{M \times N}\sum_{i=1}^{M}\sum_{j=1}^{N} o_{i,j} \tag{5}$$

$$\sigma_{i,j}^{l} = \sqrt{\frac{1}{w \times w}\sum_{i=1}^{w}\sum_{j=1}^{w}\left(o_{i,j} - m_{i,j}^{l}\right)^{2}} \tag{6}$$

Hence, we can rewrite Eq. (2) as

$$e_{i,j} = \frac{k \times m^{g}}{\sigma_{i,j}^{l} + b}\left(\left(o_{i,j} - c \times m_{i,j}^{l}\right) + \left(m_{i,j}^{l}\right)^{a}\right) \tag{7}$$

The transformation function defined in Eq. (7) stretches the contrast of the original image centered at its local mean value. A prior empirical study was undertaken to fix the window size for extracting the local information from the processed images. Thus, we have fixed a window size of 3×3 for all the images tested. The four parameters (a, b, c, k) decides the amount of stretch, capable of bringing about variations in the intensity values generated and hence need to be optimized.

3.2. Fitness criterion

Fitness function is viewed as the bottleneck of an optimization algorithm which computes the quality of an enhanced image. An automatic image enhancement approach requires a fixed fitness function independent of manual selection of parameters [8,19]. Review of the literature reveals the use of different fitness functions for various image enhancement approaches [12,17,28]. We have defined a fitness function combining the global standard deviation, entropy and edge information of the transformed image to quantify the enhancement quality. Mere multiplication of those three values would not be a good choice, since all these operands yield very small values for a processed image and their multiplication will result in still smaller value. Therefore, in order to overcome this problem we have used the geometric mean of these operands as the fitness function. The global standard deviation of an image gives the measure of dispersion of intensity values from its mean. Higher value of standard deviation depicts that the intensities in the image are spread far apart increasing the visual contrast. The use of global standard deviation alone as a fitness testing criterion may yield erroneous results since it may not be able to detect the correctly enhanced image.

Entropy value is used to reveal the information content present in an image. A uniform distribution of intensities, resulting in an equalized histogram yield higher entropy value reflecting its visual contrast. It also restricts the noise intensification, which may result in artificial images with very low intensity values. A higher value of entropy assures a wider range of intensity values in the image, contributing to the naturalness of the processed image.

In spite of the fact that the use of global operands like standard deviation and entropy facilitates in reducing the computational complexity, the use of local operands are of good choice for fitness evaluation. Edge information extraction by using algorithms like Laplacian, Canny, Sobel, etc. are of good choice to determine the extent of contrast enhancement produced in an image [1,29,30]. High contrast images definitely possess more number of detectable edges and hence a reliable and fast Sobel edge detector is been included in our fitness function [1]. The edge information is reliable in sense that, by increasing the overall edge intensity and the number of pixels defining an edge, we can obtain the enhanced version of the original image. The motivation of using this combination of global and local operands is that the use of any one them may not help in clearly distinguishing and quantifying the extend of enhancement. The use of Sobel operator alone, will help in finding an image with maximum number of edges, but fails to satisfy the global contrast in other areas. A combination of Sobel operator and standard deviation measure may result in a black and white image. Although most of the contrast stretching methods is highly sensitive to noise, the presence of an entropy measure restricts noise intensification preventing the binarization of images. Mathematical formulation of the fitness function used is given by Eqs. (8) and (9)

$$F(e) = \sqrt[3]{std_{global} \times entropy \times edge\ information} \tag{8}$$

$$\begin{aligned} F(e) &= \sqrt[3]{\sigma_e \times \log(\log(E(e^s))) \times \frac{n_{edges}(e^s) * H(e)}{M \times N}} \\ \text{where}\quad \sigma_{e_{i,j}} &= \sqrt{\frac{1}{M \times N}\sum_{i=1}^{M}\sum_{j=1}^{N}\left(e_{i,j} - m_{e_{i,j}}\right)^{2}} \\ m_{e_{i,j}} &= \frac{1}{M \times N}\sum_{i=1}^{M}\sum_{j=1}^{N} e_{i,j};\ e_{i,j}^{s} = \sqrt{\left(\nabla_x e_{i,j}\right)^{2} + \left(\nabla_y e_{i,j}\right)^{2}} \\ \nabla_x e_{i,j} &= g_{i+1,j+1} + 2g_{i+1,j} + g_{i+1,j-1} - \left(g_{i-1,j+1} + 2g_{i-1,j} + g_{i-1,j-1}\right) \\ \nabla_y e_{i,j} &= g_{i-1,j-1} + 2g_{i,j-1} + g_{i+1,j-1} - \left(g_{i-1,j+1} + 2g_{i,j+1} + g_{i+1,j+1}\right) \end{aligned} \tag{9}$$

The term $g_{i,j}$ denotes the gray level intensity value of the enhanced image 'e' specified by the coordinate values (i, j), $E(e^s)$ is the sum of all the pixel intensity values of Sobel edge detected image e^s and 'n_{edges}' gives the total number of pixels in e^s whose intensity is higher than a defined threshold value. The global entropy of enhanced image $H(e)$ is given by Eq. (10) [31].

$$H(e) = -\sum_{i=0}^{L_{\max}-1} p_e(i)\log_2(p_e(i)) \tag{10}$$

where $p_e(i)$ is the probability of occurrence of pixels with ith intensity value in the enhanced image 'e' and L_{max} is the maximum intensity value present in the enhanced image.

3.3. Parameter optimization algorithm

Evolutionary computation paradigms are basically stochastic population based methods. These methods are derived from biological adaptation models, which are apparently powerful and robust for complex optimization problems. A classical evolutionary computation model includes techniques termed as evolutionary algorithms (EAs) involving genetic programming and evolution strategies [14]. The major highlights of EAs include its capability of global search, effectiveness in handling constraints with minimum input requirements with reliable performance. These make them highly adaptable for handling complex image processing problems. The transformation function defined in Eq. (7) is used for obtaining the enhanced image in our proposed algorithm. The selection of the four parameters (a, b, c, k) in the transformation function affects the image enhancement [31].

In this paper, we propose an effective and efficient optimization algorithm for image enhancement by modifying and improving the traditional DE algorithm, by including the local search procedure of cuckoo search algorithm. Thus, the proposed MDE algorithm is used for the selection of the optimal combination of those four parameters to effectively enhance the input image. The detailed mathematical analysis and discussions of the proposed MDE algorithm is presented in the next section.

4. Proposed modified differential evolution (MDE) algorithm

Differential evolution (DE) algorithm is a robust and reasonably fast stochastic population based parallel search optimization approach proposed by Storn and Price [32]. Different variants of DE were devised by the authors based on schemes used for performing crossover and mutation of agents [33,34]. Trail vectors for the

mutation phase are generated in each of these strategies by simply summing the weighted difference between randomly selected vectors from the population. The conventional representation of each variant is in the form DE /*a* /*b* /*c*, where *a*, *b* and *c* denote a string representing the vector to be perturbed, the number of difference vectors considered for perturbation and the cross over type employed (exponential or binomial) respectively [14]. The explicit updating equations of DE makes it straight forward to implement, compared with other state-of-the-art algorithms.

Cuckoo search (CS) algorithm, developed by Yang and Deb is one among the recent metaheuristic algorithms used for global optimization, mimicking the brood parasitic behavior of certain cuckoo species [35]. The exploitation phase of CS algorithm is modeled by *Lévy* flight generation, whereas, an alien egg discovery and randomization strategy models its exploration phase. CS algorithm uses a balance combination of local and global random walks controlled by a '*switching parameter*' p_a [34].

The proposed algorithm uses the combined attributes of DE algorithm and CS algorithm for efficiently enhancing the contrast of images. CS algorithm highly depends on the parameters p_a, β and α for finding the optimal solution set [35]. Among them, p_a controls the proportion of worse nests to be discovered which in turn will decide the convergence rate of the algorithm. The conventional CS algorithm sets a fixed value for p_a during the initialization phase which is made fixed throughout the entire algorithm. The selected p_a value blindly do not ensure it to be the best for the problem considered. Hence, a value on the higher side or lower side may lead to a case were the algorithm gets converged to a non-optimal final solution.

Although CS includes a very effective exploitation (intensification) stage, which models random walks by *Lévy* flight, it fails in exploring the entire solution space effectively. Whereas, DE being a derivative free population based stochastic search method uses a vectorized mutation and crossover approaches for perturbing existing vectors, ensuring productive global exploration. The vectorized mutation approach is based on the difference vector of two randomly chosen population vectors. Whereas, the cross over operation deals with the component wise exchange of vector segments. The choice of parameters used in the exploration phase guided by DE is equally important. Extensive studies were done on the parameter sensitivity and convergence properties of differential evolution [36–40]. Theoretically DE dictates an acceptable range of $F_m \in (0, 2)$, but practical implementations stick to a choice of $F_m \in (0, 1)$. In fact, empirical observations suggest $F_m \in (0.45, 0.95)$ as a good selection range, with an initial choice of $F_m \in (0.7, 0.9)$. Similarly, C_r offers a selection range (0.1, 0.8), with an initial choice of $C_r = 0.5$.

The proposed MDE algorithm utilizes the mutation, crossover and selection strategies of DE algorithm together with *Lévy* flight generation phase of CS algorithm. The inclusion of mutation, crossover and selection strategies of DE algorithm helps in extensive exploration of the entire solution space and rapid convergence to the optimal solution. The exploitation phase modeled using *Lévy* flight generation of CS algorithm intensifies the job of finding the global optimal solutions. The optimization problem considered in this paper is to solve the complex enhancement problem defined in Section 3. The transformation function defined in Section 3.1 is used to enhance the input image. The selection for unknown parameters (*a*, *b*, *c*, *k*) considerably influence the enhanced results. Hence, the main idea of applying the proposed MDE algorithm is to search for the optimum values of those four parameters.

The detailed steps and procedures followed by the proposed MDE algorithm are as follows:

Step 1: Initialization phase: Initialization phase generates a random set of values following uniform probability distribution for the variables to be optimized by MDE algorithm, subject to its boundary constraints in a *n*-dimensional problem space. Since, our objective is to find the best quartet for the unknown parameters (*a*, *b*, *c*, *k*), *n* is fixed as 4 in our scenario. Each of those parameters are bound to some boundary constraints which is given by $a \in [0, 1.5]$, $b \in [0, 0.5]$, $c \in [0, 1]$ and $k \in [0.5, 1.5]$. $\mathbf{x}_i$ corresponds to the *i*th candidate vector in the population which denotes a parameter quartet computed using Eq. (11) with $\mathbf{x}^{min} = [0, 0, 0, 0.5]$ and $\mathbf{x}^{max} = [1.5, 0.5, 1, 1.5]$. This phase also includes the manual selection of the key parameters used in DE such as population size (N_p), mutation factor (F_m), crossover rate (C_r) and the stopping criteria for iteration (G_{max}).

$$\mathbf{x}_{i,j} = \mathbf{x}_j^{\min} + (\mathbf{x}_j^{\max} - \mathbf{x}_j^{\min})\ \ rand(n)$$
$$\text{i} = 1, 2, \ldots N_p \text{ (population size)}, \quad j = 1, 2, \ldots, n \text{ (dimension of the problem)} \tag{11}$$

Step 2: Fitness evaluation: This step evaluates the fitness of each individual using the fitness criterion defined in Eq. (9).

Step 3: Mutation operation: Mutation operation refers to the process of adding a uniform random variable to one or more vector parameters. DE algorithm depends on the population itself to provide appropriate vector increments with specific magnitude and orientation [14]. Thus a mutation operation is performed by DE which is defined in Eq. (12).

$$\mathbf{z}_{i,G+1} = \mathbf{x}_{p,G} + F_m(\mathbf{x}_{q,G} - \mathbf{x}_{r,G}) \tag{12}$$

where $\{\mathbf{x}_p, \mathbf{x}_q, \mathbf{x}_r\} \in \mathbf{x}_i$; $i = 1, 2, \ldots, N_p$ specifies the index of the individual in the population $\mathbf{x}_{i,G} = \{\mathbf{x}_{i,1,G}, \mathbf{x}_{i,2,G}, \ldots, \mathbf{x}_{i,n,G}\}$, the index 1, 2, ..., *n* specifies the position of the *i*th individual of the population. F_m controls the effect of the difference vector $(\mathbf{x}_{q,G} - \mathbf{x}_{r,G})$ in mutation operation, which will help in avoiding search stagnation.

Step 4: Crossover operation (recombination): The rate of recombination or crossover is controlled by a crossover parameter C_r. DE algorithm normally adopts two different strategies for controlling crossover, i.e. binomial crossover and exponential crossover. DE/rand/1/bin strategy uses binomial crossover scheme on each of the *n* elements or parameters as given in Eq. (13).

$$\mathbf{u}_{i,j,G+1} = \begin{cases} \mathbf{z}_{i,j,G+1} & \text{if } \ randb(j) \le C_r \\ \mathbf{x}_{i,j,G} & \text{if } \ randb(j) > C_r \end{cases} ;\ j = 1, 2, \ldots, n \tag{13}$$

where *randb*(*j*) is the *j*th evaluation of a uniform random number generator with outcome $\in$ [0,1], which ensures that $\mathbf{u}_{i,G+1}$ gets at least one parameter from $\mathbf{z}_{i,G+1}$ [32,34].

Step 5: Selection operation: Selection process is used to choose the fittest candidate by evaluating each of the possible solutions using a predefined fitness criterion. Depending on the problem to be analyzed, the objective will be to minimize or maximize the fitness function. Since, our problem is to enhance the input image by maximizing the fitness function depicted in Section 3.2, the selection operation can be defined as in Eq. (14)

$$\mathbf{x}_{i,G+1} = \begin{cases} \mathbf{u}_{i,G+1}, & \text{if } \ F(\mathbf{u}_{i,G+1}) \le F(\mathbf{x}_{i,G}) \\ \mathbf{x}_{i,G} & \text{otherwise} \end{cases} \tag{14}$$

Step 6: Lévy flight generation and solution set updation: This phase imitates the random walk pattern by generating new solution set, retaining the most fittest solution vector in the previous step. The new solution sets are generated using Eq. (15) and are updated as follows:

$$\mathbf{x}_{i,G+1} = \mathbf{x}_{i,G} + L(s, \beta),\ 0 < \beta \le 2; \quad \text{where} \quad L(s, \beta)$$
$$= \frac{\alpha\beta\Gamma(\beta)\sin(\frac{\pi\beta}{2})}{\pi \mid s\mid^{1+\beta}},\ (s \gg 0) \tag{15}$$

where *G* specifies the iteration (generation) number, *s* is the step size, α denotes the scaling factor for the step sizes generated following *Lévy* distribution and the parameter β is chosen within the range [0,2].

Lévy flights are apparently more efficient than brownian random walks in exploring large search spaces, mainly because *Lévy* flights (or walks) traces ultra-long steps, which are absent in Brownian walks. Moreover, in Brownian random walks, walker returns many times to previously visited locations which results in 'oversampling'. Whereas, the *Lévy* walker occasionally takes long jumps to the new territory. This reduction in oversampling is a part of the theoretical basis for interest in the *Lévy*-flight foraging hypothesis, which predicts that *Lévy* flights offer higher search efficiencies in environments where prey is scarce. For a β value set to 1.5, the total number of iterations required

$$\left(G_{\max} = \left(\frac{L^2}{\delta^2 d}\right)^{1/3-\beta},\ L = 10\ (scale\ of\ dimensions),\ d = 10\ \ (space\ dimension)\right)$$

to reach optimality with an accuracy error of $\delta = 10^{-5}$ can be reduced from the $O(10^{11})$ as in brute force method to $O(10^{7})$ [41,42].

A *Lévy* flight modeling requires the choice of a proper direction and magnitude of step sizes. The direction generation is done merely by drawing from uniform distribution, whereas the step size selection is mostly done using Mantegna's algorithm resulting in a symmetric and stable *Lévy* distribution, [34,35,43–45]. This will help in reducing the chance of premature convergence of solutions to an extend.

Step 7: Termination condition: The fitness of the new solution set is tested and the same steps are followed in a loop till the maximum number of iterations (G_{max}) is crossed. The final solution set which optimizes the fitness function gives the best solution for the complex problem analyzed.

The flowchart of the proposed MDE algorithm is given in Fig. 1. The modifications included in the proposed MDE algorithm over the basic DE algorithm is highlighted with blue color in the flowchart.

4.1. Illustration of proposed MDE algorithm

This subsection illustrates the effect of MDE algorithm in enhancing satellite images as compared with the basic DE and CS algorithms. It demonstrates the effectiveness of combining the exploration and exploitation phases of DE and CS algorithms respectively, in enhancing minute details present in satellite images with less artifacts. Fig. 2 gives a visual comparison between these three algorithms. The qualitative evaluation of those images proves that the proposed MDE algorithm yields the best contrast and brightness enhancement results ensuring sharpness of features with very less image distortion. The convergence plots included in Fig. 3 shows the impact of the MDE algorithm in improving the convergence rate of DE algorithm, reducing the chances for premature convergence to sub-optimal solution set. The plots also help in revealing the stability of the proposed algorithm in enhancing the tested image datasets.

5. Simulation results and discussion

In order to make a comparison on the optimization ability and enhancement quality of the proposed enhancement algorithm, studies were carried out using recent state-of-the-art remote sensing enhancement algorithms like Discrete Wavelet Transform and Singular Value Decomposition (DWT-SVD) [46], Regularized-Histogram Equalization and DCT (RHE-DCT) [47], Low Color Correction (LCC) [48,49], Tone Mapping Method (TMM) [48,50], Low-light IMage Enhancement (LIME) technique [51], Linking Synaptic Computation Network (LSCN) [52] and optimization based algorithms such as Particle Swarm Optimization (PSO) [12], Hybrid DE-SA algorithm [53], Beta Differential Evolution (BDE) [18], and adaptive Particle Swarm Optimization and Cuckoo Search algorithm (PSO-CS) [17]. This section provides the comprehensive

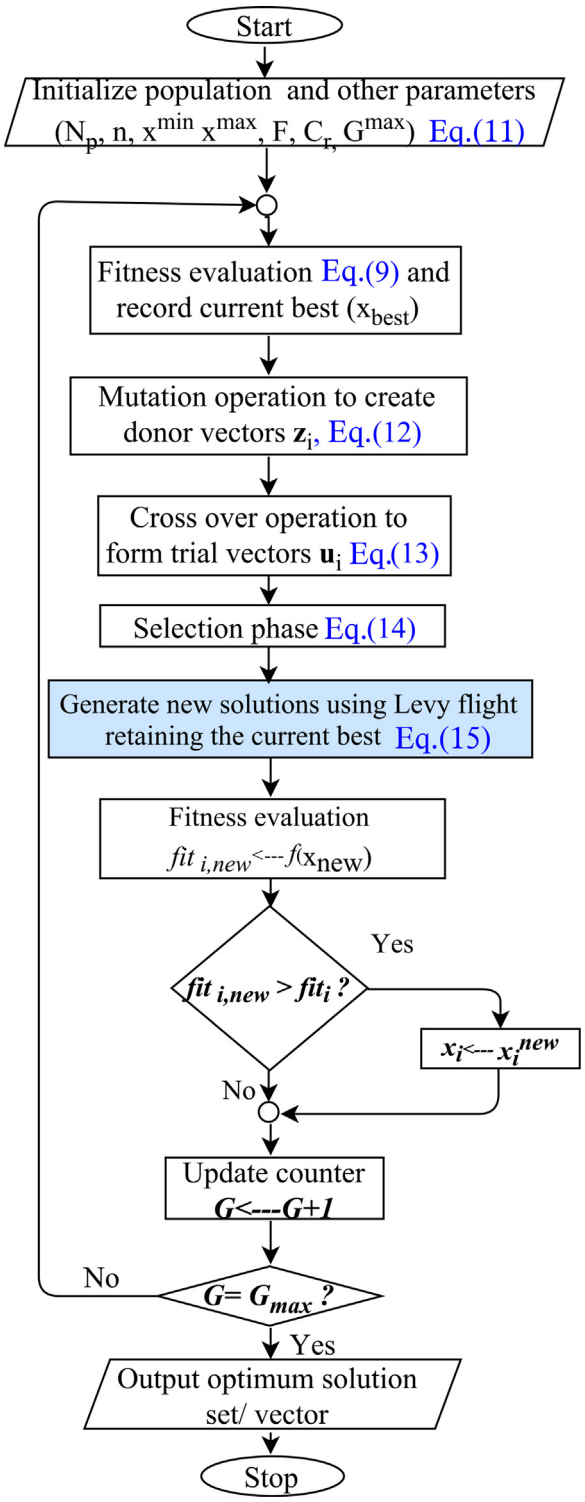

Fig. 1. Flowchart of proposed MDE algorithm.

enhancement results obtained by comparing the proposed MDE algorithm with the other existing algorithms mentioned above.

DWT-SVD technique was devised particularly for satellite image enhancement by the authors [46]. The proposed technique includes the decomposition of the input image into four sub bands using DWT, estimating singular value matrix for the LL sub band and reconstructing the enhanced image using inverse DWT.

In RHE-DCT based enhancement approach, the input image undergoes an initial global contrast enhancement stage by regular-

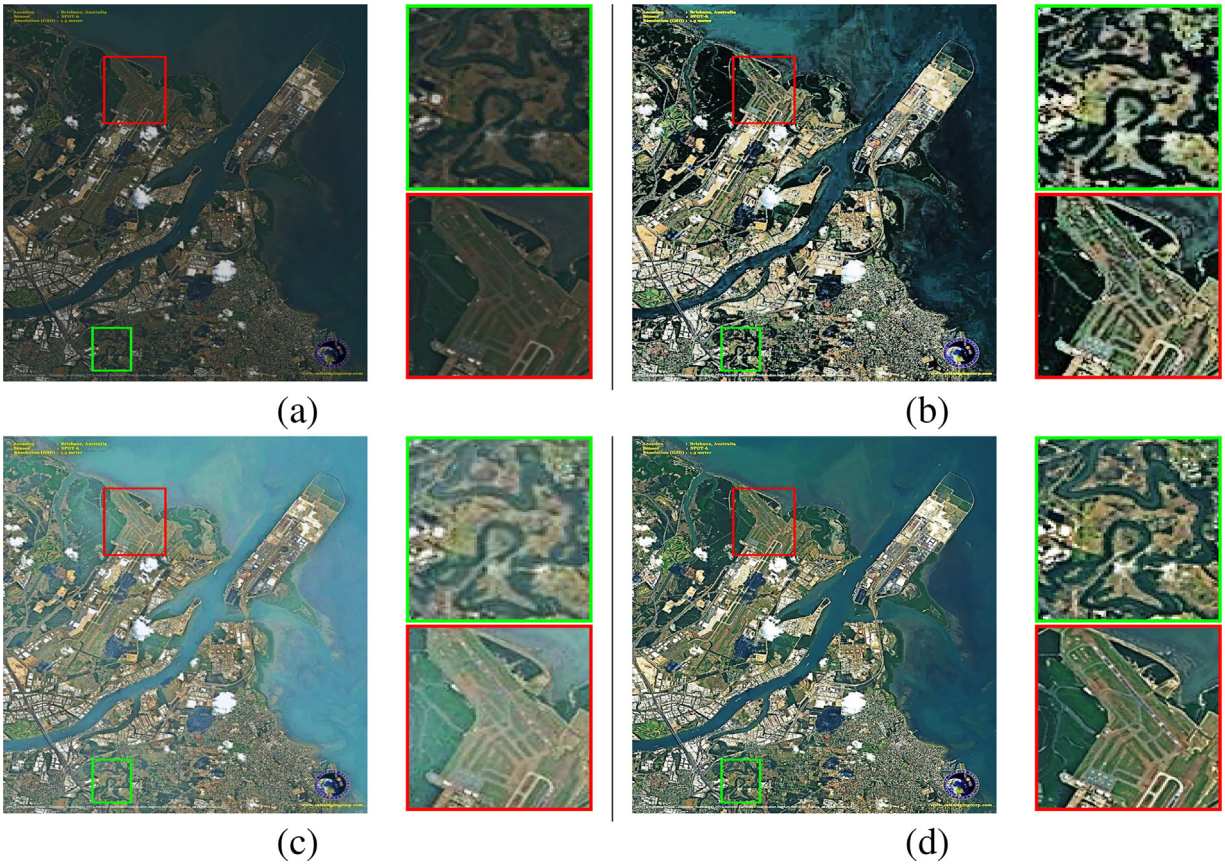

Fig. 2. Enhancement results of Image 1: (a) original, (b) DE, (c) CS and (d) proposed MDE.

izing its histogram. A sigmoid function together with the histogram is then used to generate a distribution function for the input image. Then the standard HE technique is adopted to produce a new image with improved global contrast. The DCT coefficients of this image are further adjusted automatically for enhancing the local details present in the image [47].

LCC method is an extension of Land's retinex theory which models our natural ability to see color as roughly constant with varying lighting conditions. It lessens the weaknesses of the retinex theory by focusing on the computational aspects of the problem [48,49].

TMM is a statistical approach, proposed by Mai et al. which models an appropriate tone-mapping operator (TMO), that can improve the reconstructed image quality significantly [50]. The model formulates a numerical optimization problem to find the optimum tone-curve that minimizes the expected Mean Square Error (MSE), thereby reducing the overall computational complexity [48,50].

The process of the linking synaptic computation evolved inspired by the gamma band oscillations via local coupled synaptic modulation in visual cortex. The linking synaptic mechanism allows integrating the temporal and spatial information of the network. In LSCN method, an image is fed as the input to the network and the enhanced image is obtained by the final linking synaptic state [52].

LIME is a technique particularly developed for enhancing images captured in low light conditions. This technique is built based on the model that any such captured image can be decomposed into the element-wise product of the scene albedo and the illumination (shading) images [51]. The method proceeds through an initial illumination map estimation step which iteratively gets refined, taking the benefit of local consistency, to obtain the image with enhanced details.

PSO based image enhancement algorithm works in such a way so as to maximize a defined fitness criterion, dependent on the intensity transformation function using a modified PSO algorithm [12]. The process finally yields an optimum set of transformation function dependent parameters which can provide efficient enhancement of the input image.

Beta DE algorithm also works in the similar fashion, wherein modified version of DE controls the flow of the entire algorithm. The algorithm uses an entropy based fitness function, which is maximized to yield a new set of pixel intensity values used for mapping the input image to its enhanced version [18]. Hybrid variants such as PSO-CS and DE-SA optimization algorithms also follows the aforementioned strategies for optimizing certain parameters used for image transformation [17,53]. A tricky combination of exploration and exploitation phases makes a hybrid optimization algorithm adaptable for any low contrast image enhancement problems. For a decent comparison of the results, all the above optimization algorithms were initiated with a constant population size (N_p) of 40 and were run for a fixed number of iterations (G_{max}= 100). The boundary constraints for the parameters to the optimized is set to be $a \in [0, 1.5]$, $b \in [0, 0.5]$, $c \in [0, 1]$ and $k \in [0.5, 1.5]$. The values of other parameters utilized by different optimization algorithms are given in Table 1. All the above mentioned algorithms were implemented and simulated using MATLAB R2015a running on an Intel® Core™ i7-3770 PC with 3.40 GHz CPU, 8 GB RAM and 64-bit operating system.

The proposed algorithm was tested on several images procured from NASA, Satpalda Geospatial Services and Satellite Imaging Corp. All the images chosen had low contrast in local areas, but significant illumination disparities in the global space. This paper includes the enhancement results of six satellite images and four natural images. The images chosen follows different illumination

Table 1
Parameters used in each nature inspired optimization algorithm compared.

Algorithm	Parameters	Value
PSO	Inertial weight (W), positive acceleration constants (c_1, c_2)	0.8, (1.2, 0.8)
DE-SA	Population size, maximum number of generations Scaling factor (F), crossover constant (C_r)	40, 100 0.8, 0.2
BDE	Size of population, maximum iterations Initial Weighting Factor (F), crossover rate (CR)	40,100 0.5, 0.2
PSO-CS	Dimensionality of problem (n), maximum generations (M_{gen}) Inertial weight factor (W), cognitive coefficients [C_1, C_2] of PSO Switching parameter p_a of CS Bounds of transformation function specific parameters α, β	2, 100 1, [2,2] 0.25 $\alpha \in [0, 10]$, $\beta \in [0, 10]$
Proposed MDE	Mutation factor (F), crossover probability (C_r)	0.8, 0.5

conditions which will help to clearly demonstrate the robustness of the proposed MDE algorithm. The basic information about those images are given in Table 2.

5.1. Quantitative evaluation of enhanced images

The performance of the proposed algorithm is evaluated by considering the fidelity of the processed image to the original image. We have included full-reference as well as no-reference quality metrics for quantitative performance evaluation.

5.1.1. Full-reference quality metrics for quantitative performance evaluation

Peak Signal to Noise Ratio (PSNR) is used very frequently as a quality measurement parameter which quantify the enhancement efficiency of an algorithm. PSNR value effectively gives a similarity measure of the processed image with the original image based on Mean Square Error (MSE) values computed over each pixel. So a higher PSNR value corresponding to a lower MSE is preferable.

$$PSNR(dB) = 10\log_{10}\left(\frac{L_{\max}^2}{MSE}\right);\ \text{where}\ \ MSE = \frac{1}{MN}\sum_{i=1}^{M}\sum_{j=1}^{N}[o_{i,j} - e_{i,j}]^2 \tag{16}$$

where '$M \times N$' denotes the size of the image, L_{max} is the maximum pixel intensity value and 'o' and 'e' represent the original and processed images respectively [43,54].

Another quality index measure proposed by Wang and Bovik is universally applicable to different image processing tasks [55]. Unlike the traditional error summation methods, the proposed Universal Quality Index (UQI) is designed to model an image as a combination of loss of correlation, luminance distortion, and contrast distortion factors. Hence, a higher value for this metric, quantifies an improved performance of the evaluated algorithm.

In general, if we represent the original and the processed test signal as $\mathbf{x} = \{x_i | i = 1, 2, \ldots, N\}$ and $\mathbf{y} = \{y_i | i = 1, 2, \ldots, N\}$ then UQI can be evaluated using Eq. (17).

$$\text{UQI} = \text{Loss of correlation} \times \text{Luminance distortion} \times \text{Contrast distortion factors}$$
$$\text{UQI} = \left(\frac{\sigma_{xy}}{\sigma_x\sigma_y}\right)\left(\frac{2\bar{x}\bar{y}}{(\bar{x})^2 + (\bar{y})^2}\right)\left(\frac{2\sigma_x\sigma_y}{\sigma_x^2 + \sigma_y^2}\right) = \frac{4\sigma_{xy}\bar{x}\bar{y}}{\left(\sigma_x^2 + \sigma_y^2\right)[(\bar{x})^2 + (\bar{y})^2]} \tag{17}$$

where $\bar{x} = \frac{1}{N}\sum_{i=1}^{N} x_i$, $\bar{y} = \frac{1}{N}\sum_{i=1}^{N} y_i$, $\sigma_x^2 = \frac{1}{N-1}\sum_{i=1}^{N}(x_i - \bar{x})^2$, $\sigma_y^2 = \frac{1}{N-1}\sum_{i=1}^{N}(y_i - \bar{y})^2$, $\sigma_{xy} = \frac{1}{N-1}\sum_{i=1}^{N}(x_i - \bar{x})(y_i - \bar{y})$.

So as to apply this quality index for 2D images, we apply it across local regions using sliding window technique. Starting from the top left corner of the image, the window of size $n \times n$ slides across every rows and columns, till it reaches the bottom right of the image. The computed local quality index Q_j is then combined to form the *UQI* of the entire image. If the total number of steps taken by sliding window is M, then the overall *UQI* is computed using Eq. (18).

$$Q = \frac{1}{M}\sum_{j=1}^{M} Q_j \tag{18}$$

Feature Similarity Index (FSIM) is the quality metric which gives the measure of feature similarity between the original and processed image [56]. The value ranges from 0 to 1 and a higher FSIM value indicates improved capability of the evaluated algorithm in preserving relevant features. It can be mathematically formulated as given in Eq. (19)

$$FSIM = \frac{\sum_{x \in I} S(x) PC_m(x)}{\sum_{x \in I} PC_m(x)} \tag{19}$$

where I represents the entire image, $S(x)$ denotes the similarity between the two images under consideration and PC_m is the phase congruency map for original as well as processed image. $m \in (0, 1)$ where $m = 0$ refers to the original image and $m = 1$ refers to the processed (enhanced) image [57].

Normalized Absolute Error (NAE) is a measure used to indicate the efficiency of transformation modeled for an image [58]. A good transformation yield very small difference (error) between the original image preserving relevant details. The index is mathematically formulated using Eq. (20) given below

$$NAE = \frac{\sum_{i=1}^{M}\sum_{j=1}^{N}|e_{i,j} - o_{i,j}|}{\sum_{i=1}^{M}\sum_{j=1}^{N}|o_{i,j}|} \tag{20}$$

where $o_{i,j}$ and $e_{i,j}$ represents the intensity values of (i, j)th pixel of the original and processed (enhanced) image receptively.

Structural Contrast-Quality Index (SC-QI): is a recent full reference image quality assessment method devised by Bae et al., which can well characterize local and global visual quality perceptions [59].

The detail analysis of the steps included in computing SC-QI score is given in [60]. The overall SC-QI score of an image can be thus calculated using Eq. (21).

$$SC - QI_{(o,e)} = \frac{1}{W}\sum_{m=1}^{B} w(\mathbf{o}^{(m)}, \mathbf{e}^{(m)})\, f(\mathbf{o}^{(m)}, \mathbf{e}^{(m)}) \tag{21}$$

where $\mathbf{o}$ and $\mathbf{e}$ are the input and output images in luminance (L), chrominance (M, N) color space, $w(\mathbf{o}, \mathbf{e})$ is the local weight based on visual priors with respect to its local importance (e.g., degree of image content information, phase congruency, visual saliency index, etc.). $f(\mathbf{o}, \mathbf{e})$ are the computed local features and W is a normalization factor which is calculated as the summation of all $w(\mathbf{o}, \mathbf{e})$ values over all B local image blocks. The SC-QI metric value

Table 2
Basic information about the images used for evaluation.

Image	Basic information		Image	Basic information	
 Image 1	Size	793×624	 Image 2	Size	900 × 792
	[Min, Max]	R[0,229], G[0,225], B[0,226]		[Min, Max]	R[0,158], G[0,152], B[0,155]
	Source	http://www.satimagingcorp.com/gallery/		Source	http://www.satpalda.com/gallery/pleiades-imagery/
 Image 3	Size	1200 × 1200	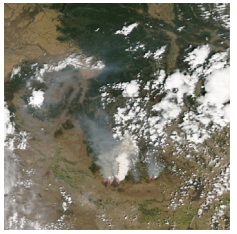 Image 4	Size	1800 × 2400
	[Min, Max]	R[0,255], G[0,255], B[0,255]		[Min, Max]	R[0,255], G[0,255], B[0,255]
	Source	http://www.satpalda.com/gallery/pleiades-imagery/		Source	https://earthobservatory.nasa.gov/
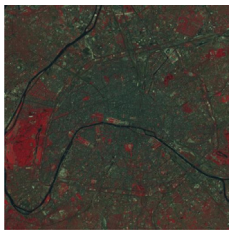 Image 5	Size	512 × 512	 Image 6	Size	984 × 768
	[Min, Max]	R[0,195], G[0,205], B[0,196]		[Min, Max]	R[0,255], G[0,255], B[0,255]

Table 2 (*Continued*)

Image	Basic information		Image	Basic information	
	Source	http://visibleearth.nasa.gov/		Source	http://www.satpalda.com/gallery/pleiades-imagery/
 Image 7	Size	1321 × 2000	 Image 8	Size	624 × 491
	[Min, Max]	R[0,255], G[0,255], B[0,255]		[Min, Max]	R[0,255], G[0,250], B[0,250]
	Source	http://dragon.larc.nasa.gov/retinex/		Source	http://dragon.larc.nasa.gov/retinex/
 Image 9	Size	1312 × 2000	 Image 10	Size	2000 × 1312
	[Min, Max]	R[3,255], G[5,255], B[2,255]		[Min, Max]	R[0,242], G[0,255], B[0,237]
	Source	http://dragon.larc.nasa.gov/retinex/		Source	http://dragon.larc.nasa.gov/retinex/

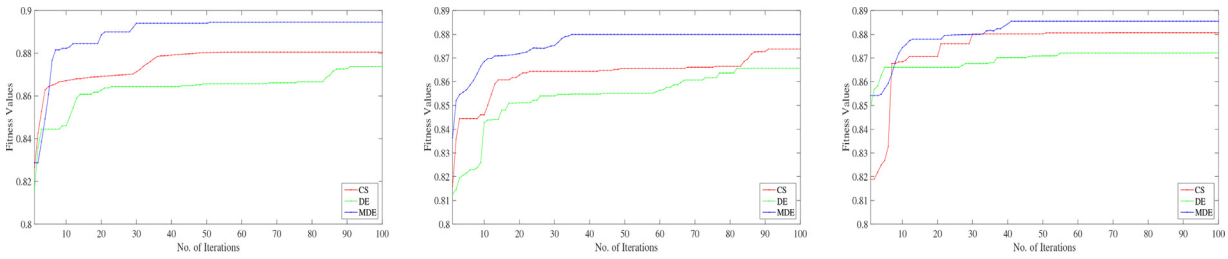

Fig. 3. Convergence analysis between DE, CS and MDE algorithms: (a) R channel, (b) G channel and (c) B channel.

Table 3
PSNR value comparison between results obtained using different enhancement algorithms.

Images	DWT-SVD Demirel et al. [46]	RHE-DCT Fu et al. [47]	LIME Guo et al. [51]	LCC Lisani et al. [48]	TMM Lisani et al. [48]	LSCN Zhan et al. [52]	PSO Gorai et al. [12]	DE-SA Gogna et al. [53]	BDE Bhandari et al. [18]	PSO-CS Ye et al. [17]	Proposed MDE
Image 1	10.8123	24.963	9.1266	25.2495	16.1343	20.9916	18.2595	20.7903	19.8326	19.4691	**25.8649**
Image 2	9.2829	15.5331	18.1415	13.4596	13.4596	19.0729	18.0718	21.3029	20.6767	18.7597	**35.2544**
Image 3	9.7755	21.2863	7.2308	12.2707	9.2671	12.2531	6.3875	11.4398	21.806	8.5598	**22.0695**
Image 4	19.8207	22.2744	9.2678	26.0241	17.398	16.6532	20.9517	18.1186	14.4371	14.0162	**26.1635**
Image 5	9.7755	21.2863	7.6743	20.2591	11.791	21.4112	18.2712	18.8204	21.6801	18.2614	**32.0773**
Image 6	12.7202	27.4828	8.0989	16.9487	8.6197	19.7742	10.3453	8.8202	21.6801	7.4973	**34.6009**
Image 7	17.0357	35.442	9.7297	18.8422	10.1208	29.0033	19.6391	21.3257	23.375	18.4405	**37.7713**
Image 8	15.0475	22.9659	8.3202	19.0749	11.0532	11.4425	18.3595	16.17	18.9753	15.9873	**24.4423**
Image 9	13.7429	28.5517	8.276	17.6919	9.9455	22.9242	12.2272	15.9281	21.7848	15.3411	**33.0016**
Image 10	12.7765	20.9947	7.2771	18.0639	10.9012	14.3571	18.658	21.0919	19.9683	19.3175	**25.7969**

Table 4
MSE value comparison between results obtained using different enhancement algorithms.

Images	DWT-SVD Demirel et al. [46]	RHE-DCT Fu et al. [47]	LIME Guo et al. [51]	LCC Lisani et al. [48]	TMM Lisani et al. [48]	LSCN Zhan et al. [52]	PSO Gorai et al. [12]	DE-SA Gogna et al. [53]	BDE Bhandari et al. [18]	PSO-CS Ye et al. [17]	Proposed MDE
Image 1	5393.1972	207.3882	7950.9809	194.1463	1583.6011	517.517	970.8102	542.0694	675.7969	734.8009	**168.4978**
Image 2	7669.9401	1818.7262	997.5504	2931.7386	2931.7386	804.9927	1013.6873	481.7146	556.4262	865.1784	**19.3928**
Image 3	6847.4258	483.5563	12302.8187	3854.9046	7697.9253	3870.5193	14939.4071	4667.6223	429.0188	9059.3991	**403.7712**
Image 4	677.6634	385.162	7696.613	162.4326	1183.7974	1405.276	522.2838	1002.8068	2340.8283	2579.035	**157.3001**
Image 5	6847.4258	483.5563	11108.3203	612.5911	4305.0804	469.8535	968.1956	853.1877	441.6401	970.3823	**40.3038**
Image 6	3475.8729	116.092	10073.6511	1312.8328	8935.2244	684.9599	6005.5113	8532.1877	441.6401	11570.3823	**22.5419**
Image 7	1286.8017	18.5731	6920.0662	848.9135	6324.0981	81.7993	706.6004	479.1967	298.9382	931.1786	**10.863**
Image 8	2033.9094	328.4638	9573.292	804.6149	5102.2045	4664.7676	948.6961	1570.6358	823.2847	1638.1315	**233.8007**
Image 9	2746.5799	90.7628	9671.2245	1106.3566	6584.5797	331.6362	3893.6476	1660.6229	431.1236	1900.9484	**32.5779**
Image 10	3431.0929	517.1379	12172.3244	1015.5189	5283.9232	2384.3595	885.685	505.6974	655.0063	760.8977	**171.1556**

Table 5
UQI value comparison between results obtained using different enhancement algorithms.

Images	DWT-SVD Demirel et al. [46]	RHE-DCT Fu et al. [47]	LIME Guo et al. [51]	LCC Lisani et al. [48]	TMM Lisani et al. [48]	LSCN Zhan et al. [52]	PSO Gorai et al. [12]	DE-SA Gogna et al. [53]	BDE Bhandari et al. [18]	PSO-CS Ye et al. [17]	Proposed MDE
Image 1	0.5446	0.9729	0.6662	0.9766	0.9001	0.9793	0.9624	0.8223	0.8841	0.8779	**0.9823**
Image 2	0.3946	0.7205	0.9463	0.84	0.84	0.9185	0.7623	0.6539	0.6734	0.6733	**0.9671**
Image 3	0.4768	0.9416	0.3617	0.6141	0.4904	0.6462	0.3694	0.5594	0.7815	0.455	**0.9633**
Image 4	0.9686	0.9555	0.7045	0.9901	0.9492	0.9425	0.9808	0.9792	0.6559	0.8755	**0.9948**
Image 5	0.4768	0.9416	0.3884	0.8384	0.6377	0.9434	0.4822	0.4786	0.6299	0.4092	**0.999**
Image 6	0.6149	0.9353	0.3755	0.6666	0.3776	0.799	0.5065	0.4786	0.6299	0.4092	**0.9648**
Image 7	0.468	0.7159	0.2209	0.3792	0.2036	0.6341	0.2164	0.2485	0.266	0.2322	**0.7324**
Image 8	0.8638	0.8155	0.5978	0.8993	0.7003	0.7184	0.9443	0.9038	0.8121	0.8975	**0.9846**
Image 9	0.6555	0.5842	0.3868	0.646	0.4246	0.8041	0.5763	0.7444	0.6009	0.6496	**0.9242**
Image 10	0.5932	0.8653	0.2768	0.8121	0.5569	0.7244	0.4768	0.472	0.735	0.381	**0.8892**

ranges between 0 and 1. The higher its value, the better will be the performance of the algorithm.

5.1.2. No-reference quality metrics for quantitative performance evaluation

We also assess the contrast enhancement performance objectively using three no-reference quality metrics, which includes Discrete Entropy [6,61,62] Michelson Constant ($C_{Michelson}$) [47,63] and Colorfulness Metric (CM) [64,65].

Discrete Entropy is a measure which is used to quantify the information content of an image [61]. Low entropy images, possesses very little contrast and large number of pixels with the same intensity values and vise versa. Hence DE can be included as an

Table 6
FSIM value comparison between results obtained using different enhancement algorithms.

Images	DWT-SVD Demirel et al. [46]	RHE-DCT Fu et al. [47]	LIME Guo et al. [51]	LCC Lisani et al. [48]	TMM Lisani et al. [48]	LSCN Zhan et al. [52]	PSO Gorai et al. [12]	DE-SA Gogna et al. [53]	BDE Bhandari et al. [18]	PSO-CS Ye et al. [17]	Proposed MDE
Image 1	0.8154	0.9227	0.8531	0.9596	0.9276	0.9418	0.8272	0.8596	0.7325	0.8632	**0.9902**
Image 2	0.7502	0.8079	0.7523	0.8254	0.8254	0.8643	0.8493	0.8588	0.7102	0.8896	**0.9797**
Image 3	0.7693	0.7628	0.713	0.7735	0.6032	0.6687	0.7149	0.895	0.9154	0.6575	**0.9318**
Image 4	0.9516	0.9356	0.867	0.9547	0.9217	0.9191	0.9617	0.9201	0.8462	0.8975	**0.9845**
Image 5	0.7693	0.7628	0.6903	0.9432	0.8571	0.9084	0.7526	0.8068	0.8225	0.7388	**0.9696**
Image 6	0.8419	0.9598	0.6999	0.9369	0.8104	0.9026	0.8109	0.8114	0.9061	0.7388	**0.9603**
Image 7	0.9091	0.9931	0.6643	0.9171	0.7401	0.9469	0.8675	0.7483	0.641	0.7925	**0.9962**
Image 8	0.9444	0.9581	0.832	0.97	0.93	0.9105	0.9447	0.9439	0.9599	0.9234	**0.9857**
Image 9	0.8721	0.9669	0.7599	0.9297	0.8368	0.9348	0.9072	0.9031	0.8898	0.93	**0.9851**
Image 10	0.8592	0.8798	0.7312	0.9506	0.7996	0.8738	0.7679	0.7261	0.7852	0.7428	**0.9894**

Table 7
NAE value comparison between results obtained using different enhancement algorithms.

Images	DWT-SVD Demirel et al. [46]	RHE-DCT Fu et al. [47]	LIME Guo et al. [51]	LCC Lisani et al. [48]	TMM Lisani et al. [48]	LSCN Zhan et al. [52]	PSO Gorai et al. [12]	DE-SA Gogna et al. [53]	BDE Bhandari et al. [18]	PSO-CS Ye et al. [17]	Proposed MDE
Image 1	1.2216	0.1968	0.8498	0.102	0.3214	0.1532	0.2549	0.3765	0.9	0.4152	**0.095**
Image 2	1.6821	0.7181	1.4658	0.4906	0.4906	0.2499	0.6286	0.3998	0.8546	0.7968	**0.0473**
Image 3	1.4976	0.3179	1.9662	1.0754	1.4889	0.9903	2.1523	1.2328	0.362	1.6439	**0.3161**
Image 4	0.1979	0.1366	0.726	0.0942	0.2767	0.2697	0.1628	0.2288	0.3648	0.3829	**0.0775**
Image 5	1.4976	0.3179	1.6101	0.3325	0.8935	0.2579	1.29	0.9594	0.9061	1.6342	**0.0793**
Image 6	0.9009	0.152	1.6084	0.6027	1.5464	0.3939	1.1563	1.4425	0.3225	1.6342	**0.0615**
Image 7	0.5996	0.0818	1.954	0.6438	1.6297	0.1461	1.9314	1.1845	0.8773	2.0245	**0.0652**
Image 8	0.4618	0.1665	1.0352	0.297	0.7789	0.7352	0.2831	0.3735	0.277	0.3611	**0.1432**
Image 9	0.7001	0.1278	1.422	0.4958	1.2267	0.2464	0.8725	0.4837	0.287	0.6039	**0.0712**
Image 10	0.8994	0.5152	2.2865	0.5343	1.1966	0.7571	1.2814	1.0824	0.9652	1.7309	**0.2038**

Table 8
SC-QI value comparison between results obtained using different enhancement algorithms.

Images	DWT-SVD Demirel et al. [46]	RHE-DCT Fu et al. [47]	LIME Guo et al. [51]	LCC Lisani et al. [48]	TMM Lisani et al. [48]	LSCN Zhan et al. [52]	PSO Gorai et al. [12]	DE-SA Gogna et al. [53]	BDE Bhandari et al. [18]	PSO-CS Ye et al. [17]	Proposed MDE
Image 1	0.9994	0.9976	0.9966	0.999	0.9987	0.9981	0.9979	0.9941	0.9981	0.9995	**0.9996**
Image 2	0.997	0.9979	0.9964	0.9916	0.9916	0.996	0.9887	0.9932	0.9974	0.9899	**0.9988**
Image 3	0.9964	0.9948	0.9947	0.9969	0.9922	0.9957	0.9821	0.9877	0.989	0.9879	**0.9975**
Image 4	0.9984	0.9965	0.9971	0.9984	0.9981	0.997	0.9984	0.9969	0.9957	0.9851	**0.9984**
Image 5	0.9972	0.9917	0.9919	0.9989	0.9969	0.9987	0.9962	0.9973	0.9972	0.9962	**0.9992**
Image 6	0.9975	0.9931	0.9933	0.9991	0.9967	0.9986	0.9916	0.9888	0.9983	0.9913	**0.9995**
Image 7	0.9978	0.9878	0.988	0.9982	0.9925	0.9992	0.9934	0.9925	0.9978	0.9942	**0.9995**
Image 8	0.9989	0.9971	0.9965	0.9986	0.9988	0.9982	0.999	0.9973	0.9988	0.9992	**0.9992**
Image 9	0.9961	0.9977	0.9935	0.9987	0.9959	0.999	0.9818	0.9959	0.998	0.9952	**0.9998**
Image 10	0.9972	0.996	0.9935	0.9988	0.9966	0.9968	0.9933	0.9915	0.9987	0.9827	**0.9991**

Table 9
H value comparison between results obtained using different enhancement algorithms.

Images	DWT-SVD Demirel et al. [46]	RHE-DCT Fu et al. [47]	LIME Guo et al. [51]	LCC Lisani et al. [48]	TMM Lisani et al. [48]	LSCN Zhan et al. [52]	PSO Gorai et al. [12]	DE-SA Gogna et al. [53]	BDE Bhandari et al. [18]	PSO-CS Ye et al. [17]	Proposed MDE
Image 1	7.437	7.7548	7.1439	7.3801	7.6456	7.785	7.6111	7.8007	7.4438	7.7864	**7.8252**
Image 2	7.5371	7.5425	7.1521	7.6593	7.6593	7.8219	7.7299	7.503	6.9612	7.7665	**7.9346**
Image 3	6.8093	6.8536	7.2349	7.0239	6.6847	7.4484	7.3858	6.5628	5.7643	7.3862	**7.9384**
Image 4	7.6754	7.8205	7.0535	7.534	7.7546	7.8146	7.7563	7.9105	6.2745	7.7584	**7.9741**
Image 5	7.5398	7.4531	7.3821	6.9428	7.553	7.5042	7.6443	7.5487	5.9272	7.6344	**7.781**
Image 6	7.5095	7.2353	7.6813	6.9182	7.3322	7.2688	7.7279	7.7007	4.8261	7.7326	**7.7787**
Image 7	6.6606	6.499	7.5675	6.6432	6.8446	6.4929	7.3122	7.3983	3.2109	6.8679	**7.8668**
Image 8	7.7296	7.7342	7.3209	7.3125	7.5182	7.5435	7.7468	7.7927	6.8517	7.7475	**7.8296**
Image 9	7.398	7.4825	7.6622	7.2827	7.4335	7.4892	7.7956	7.5339	5.6265	7.7078	**7.8873**
Image 10	7.2083	6.823	7.3537	6.7979	6.8472	7.2639	7.2872	7.4186	5.6735	7.6576	**7.7568**

appropriate measure to evaluate the effective contrast of an image. It is mathematically defined as given in Eq. (22)

$$H(e) = -\sum_{i=0}^{L_{\max}-1} p_e(i)\,\log_2(p_e(i)) \tag{22}$$

where $p_e(i)$ is the probability of occurrence of pixels with ith intensity value in the enhanced image 'e' and L_{max} is the maximum intensity value present in the enhanced image.

Michelson Constant ($C_{Michelson}$) gives the local contrast measure of an image evaluated using a 3×3 sliding window [63]. A higher

Table 10
$C_{Michelson}$ value comparison between results obtained using different enhancement algorithms.

Images	DWT-SVD Demirel et al. [46]	RHE-DCT Fu et al. [47]	LIME Guo et al. [51]	LCC Lisani et al. [48]	TMM Lisani et al. [48]	LSCN Zhan et al. [52]	PSO Gorai et al. [12]	DE-SA Gogna et al. [53]	BDE Bhandari et al. [18]	PSO-CS Ye et al. [17]	Proposed MDE
Image 1	0.8398	0.9558	0.7485	0.9326	0.8974	0.9951	0.8467	0.9987	0.9769	0.9215	**0.9992**
Image 2	0.7239	0.9271	0.6578	0.8715	0.8715	0.9957	0.8329	0.5915	0.9425	0.8303	**0.9989**
Image 3	0.6298	0.9875	0.6178	0.9412	0.9217	0.9903	0.5259	0.5516	0.9699	0.6818	**0.9921**
Image 4	0.7455	0.9484	0.5902	0.9387	0.9457	**0.9758**	0.7976	0.9601	0.9235	0.7039	0.9707
Image 5	0.7658	0.9126	0.5984	0.7673	0.8279	0.9398	0.7839	0.7095	0.9673	0.7245	**0.9783**
Image 6	0.8956	0.9779	0.846	0.7847	0.8371	**0.9884**	0.8592	0.7417	0.9022	0.8392	0.9842
Image 7	0.9494	0.96	0.8316	0.9032	0.8943	0.9881	0.5482	0.7548	0.9847	0.3166	**0.9885**
Image 8	0.9637	0.9908	0.9617	0.9619	0.9384	0.9912	0.9881	0.9804	0.9423	0.969	**0.9988**
Image 9	0.9312	0.9741	0.8378	0.879	0.8837	0.9929	0.7427	0.8995	0.9321	0.8504	**0.9941**
Image 10	0.6941	0.9483	0.7056	0.9737	0.8461	0.9918	0.8247	0.8084	0.9877	0.9044	**0.9919**

value of this constant indicates better contrast for the evaluated image. It is defined as given in Eq. (23)

$$C_{Michelson} = \frac{\max(e) - \min(e)}{\max(e) + \min(e)} \tag{23}$$

where '$min(e)$' and '$max(e)$' represents the minimum and maximum pixel intensity values in the 3×3 window of the processed image, respectively.

Colorfulness is yet another important attribute which can be used to measure the quality of a colored image. A no-reference metric was introduced in 2003 by Susstrunk and Winkler for evaluating the diversity and contrast of the colors present in an image and was termed as 'Colorfulness Metric (CM)' [64]. It is mathematically formulated as given in Eq. (24).

$$CM(e) = \sqrt{\sigma_{\alpha_e}^2 + \sigma_{\beta_e}^2} + 0.3\sqrt{\mu_{\alpha_e}^2 + \mu_{\beta_e}^2} \tag{24}$$

where $\alpha = R - G$ and $\beta = \frac{R+G}{2} - B$. σ and μ represent the standard deviation and mean of respective values α and β. Subscript 'e' with each parameter refers to the enhanced image. Hence, the higher its value, the better will be the performance of the algorithm.

Tables 3–11 furnishes the results obtained on comparing all the above metric values for the 11 different enhancement algorithms specified, tested over the given image dataset. The best result in each case is bolded and the second best results are underlined. Evaluation of the above specified metric values for all the algorithms compared, indicates that the proposed algorithm outperforms others to a great extend. The PSNR values obtained for all the images compared, indicates the quality of the processed image is well enhanced with respect to the original image using the proposed technique. MSE and NAE evaluation gives very small values for the proposed MDE algorithm indicating its efficiency in optimizing the parameters used for intensity transformation process. UQI, being a highly acceptable metric for evaluating the performance of an algorithm, indicates the proposed MDE algorithm to take a decent upper-hand over the others, consistently for all the satellite images and natural images considered. FSIM comparison reveals that the proposed MDE algorithm is very efficient in conserving the prominent features present in the original image making it well adaptable for further feature related processing tasks. A higher value for SC-QI metric for the proposed MDE algorithm proves its capability in enhancing the local and global visual features of the image. Comparing the no-reference performance metrics like Discrete Entropy, $C_{Michelson}$ and CM also reveal the improved performance of the proposed MDE algorithms compared with other state-of-the-art algorithms compared.

5.2. Visual evaluation of enhanced images

The subjective evaluation of the processed images using all the 11 enhancement algorithms are given in Figs. 4–13

. It clearly indicates that our proposed MDE algorithm efficiently enhances every minor details in the image reducing image artifacts. It also proved to be efficient in preserving the mean intensity of those images, thereby preserving its naturalness. The results also highlight the robustness of the proposed algorithm, making it equally applicable for satellite images as well as other natural images.

5.3. Computational complexity analysis

Computational complexity of all the above mentioned algorithms for enhancing images of size $M \times N$ was statistical analyzed. DWT-SVD algorithm accounts for an overall complexity level of $O(4MN^2 \log 2N)$. Whereas, for RHE-DCT algorithm the time complexity is computed to be in the order of $O(N \log N)$. LCC method reduced the computational complexity of Lands retinex algorithm dramatically from $O(N^4)$ to $O(N^2)$, where $N \times N$ is the dimension of processing area.LSCN is efficient with computational complexity of order $O(Rw^2MN)$, where R is the total number of iterations, $w \times w$ filter window size to output the same dynamic range with the input image. The algorithm includes a threshold initialization step which requires the calculation of local mean and variance values with a window size 3×3. This accounts for a computational

Table 11
CM value comparison between results obtained using different enhancement algorithms.

Images	DWT-SVD Demirel et al. [46]	RHE-DCT Fu et al. [47]	LIME Guo et al. [51]	LCC Lisani et al. [48]	TMM Lisani et al. [48]	LSCN Zhan et al. [52]	PSO Gorai et al. [12]	DE-SA Gogna et al. [53]	BDE Bhandari et al. [18]	PSO-CS Ye et al. [17]	Proposed MDE
Image 1	22.43370654	25.0362451	21.26432266	23.55693053	22.60735565	24.25152697	25.06921645	34.50341873	24.95051959	29.83687366	**36.41136085**
Image 2	72.8037625	47.77665	65.76425	32.719025	25.938725	28.4463875	51.2687375	35.6752125	39.69155	46.652425	**74.6561125**
Image 3	44.1720812	32.45372	59.3552856	56.7263008	43.7564868	43.4879848	42.6661352	47.2400084	24.667162	41.5080744	**59.6704836**
Image 4	9.89118771	15.09840222	15.5786577	17.85097761	11.94413166	16.62958713	17.93991381	12.72380568	17.21508378	13.85033088	**17.97697056**
Image 5	35.01396087	25.725147	50.8580604	22.80839652	24.67578309	22.86206769	42.38356773	45.65010618	21.86082276	49.46816217	**54.60578865**
Image 6	37.03627642	26.35770241	39.80504736	28.97693253	30.0667679	30.78275122	39.73480849	55.88748282	26.76327524	60.56176633	**62.2633596**
Image 7	25.62065746	17.11980161	37.33420593	21.70751373	30.41057833	17.06156549	23.26856528	47.61449878	18.30393605	36.37169228	**49.41496549**
Image 8	20.2212836	17.087049	20.498023	19.73055385	17.47802385	18.5898083	16.42577055	15.89803495	18.599462	17.13049065	**21.6757744**
Image 9	21.44719708	26.88717116	26.09301436	22.01055206	18.03728632	28.07840636	26.1699483	26.2940353	28.16030378	26.00615346	**28.6020535**
Image 10	32.13611394	22.84244247	56.81254947	32.17145856	42.99083946	33.46546437	56.39037762	47.35982721	22.27103778	52.17454989	**57.8669973**

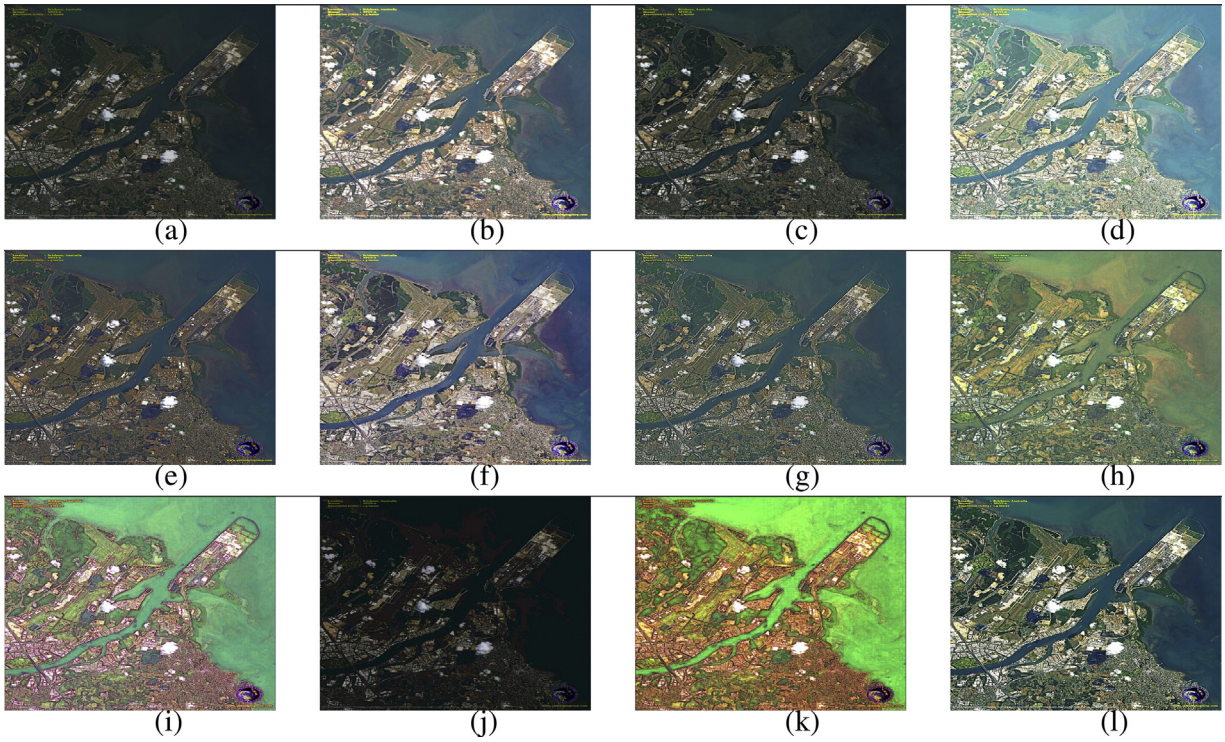

Fig. 4. Enhancement results of Image 1: (a) original, (b) DWT-SVD, (c) RHE-DCT, (d) LIME, (e) LCC, (f) TMM, (g) LSCN, (h) PSO, (i) DE-SA, (j) BDE, (k) PSO-CS and (l) proposed MDE.

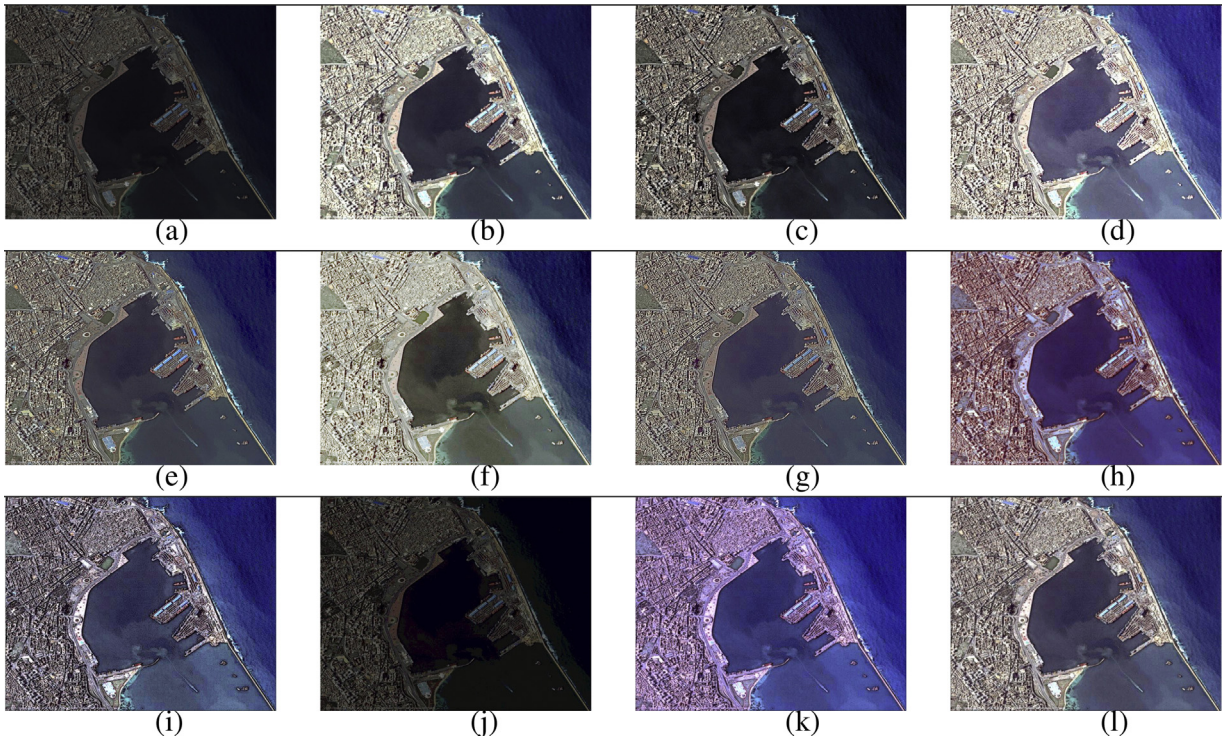

Fig. 5. Enhancement results of Image 2: (a) original, (b) DWT-SVD, (c) RHE-DCT, (d) LIME, (e) LCC, (f) TMM, (g) LSCN, (h) PSO, (i) DE-SA, (j) BDE, (k) PSO-CS and (l) proposed MDE.

complexity of $O(2 \times 3^2 MN)$. The final step for gray level stretching includes computation of the image histogram with a complexity $O(MN)$. Thus, the overall complexity of LSCN algorithm for image enhancement accounts for a computational complexity of order $O(Rw^2 MN + 19MN)$.

LIME algorithm is computationally much simpler which requires a computational time of the order $O(MN)$. Metaheuristic algorithms normally are computationally more complex compared with other classical approaches, but they are more potent in evolving optimum solutions for a complex optimization prob-

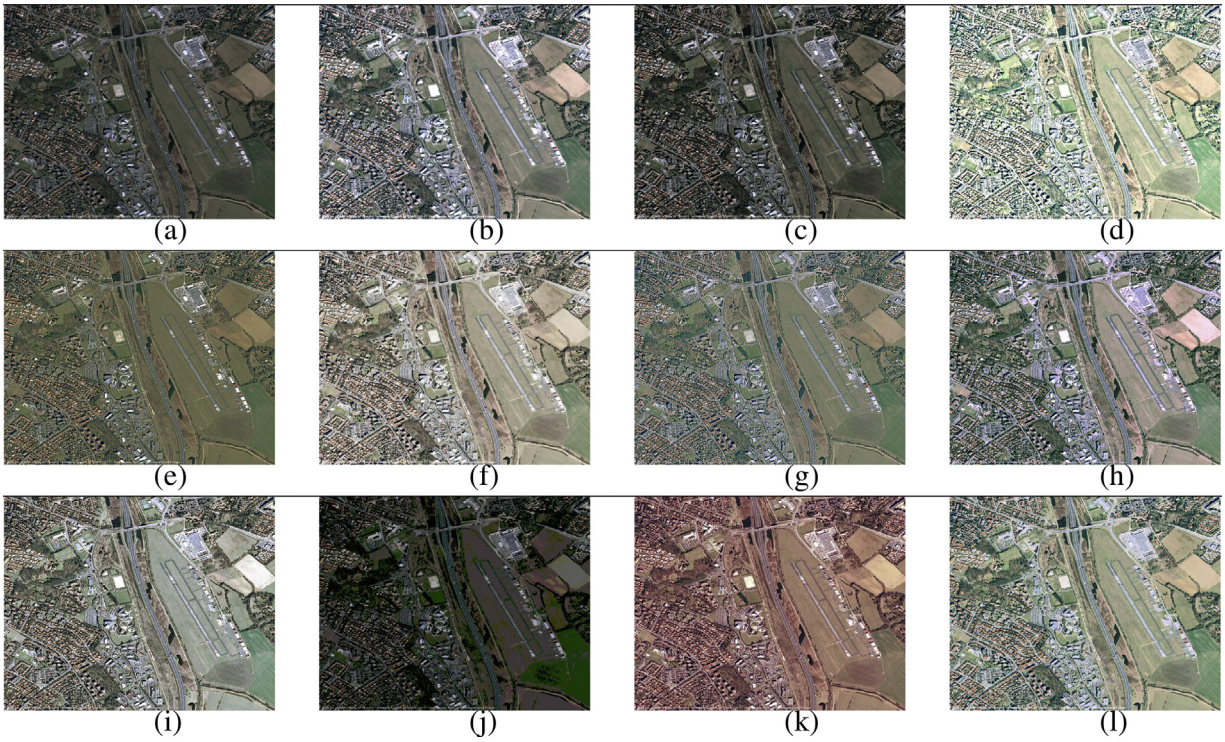

Fig. 6. Enhancement results of Image 3: (a) original, (b) DWT-SVD, (c) RHE-DCT, (d) LIME, (e) LCC, (f) TMM, (g) LSCN, (h) PSO, (i) DE-SA, (j) BDE, (k) PSO-CS and (l) proposed MDE.

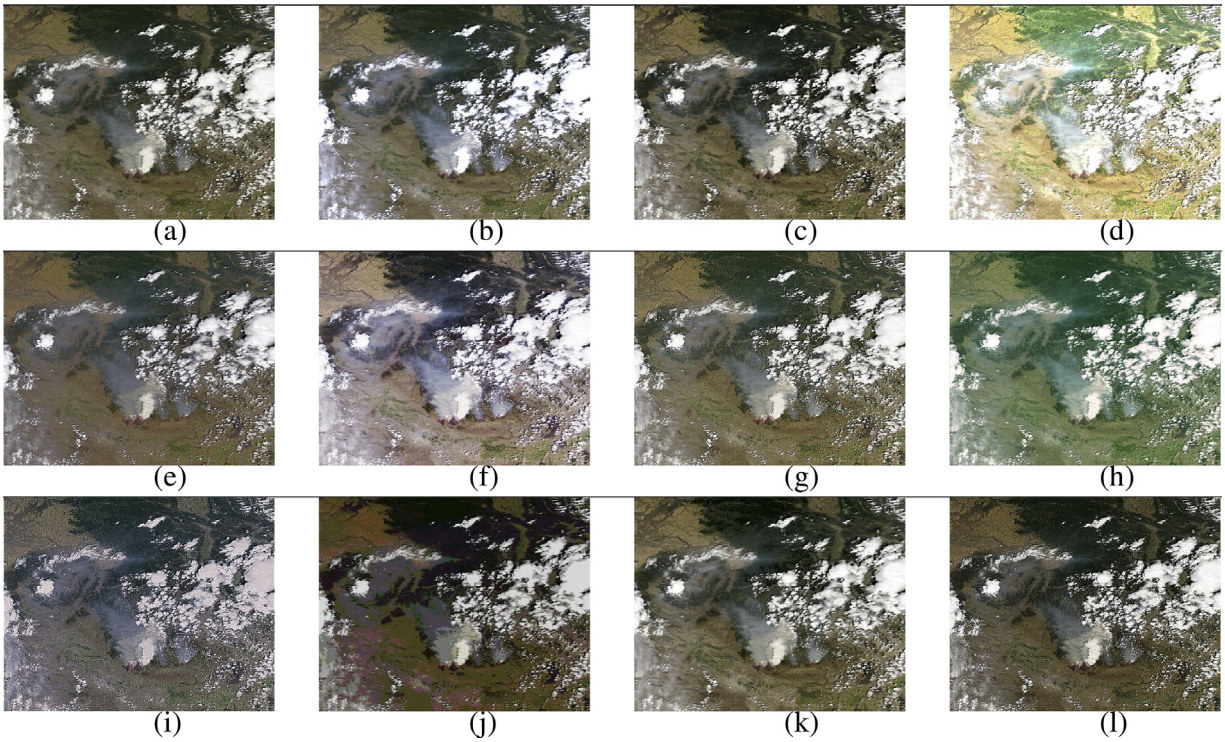

Fig. 7. Enhancement results of Image 4: (a) original, (b) DWT-SVD, (c) RHE-DCT, (d) LIME, (e) LCC, (f) TMM, (g) LSCN, (h) PSO, (i) DE-SA, (j) BDE, (k) PSO-CS and (l) proposed MDE.

lem considered. The asymptotic computational complexity of PSO algorithm was evaluated to be of the order $O(PX)$ where P is the population size and X is the total number of iterations. DE-SA algorithm is even more computationally complex and hence much slower, since the SA phase contributes to the algorithmic complexity with an order of $O(P^2)$. Whereas combination of PSO-CS and the proposed MDE algorithm yield an algorithm complexity of the order $O(PX)$, where P is decided by the initial number of random solutions chosen and dimensionality of the problem. Although the algorithmic complexity of most of the metaheuristic algorithms are obtained

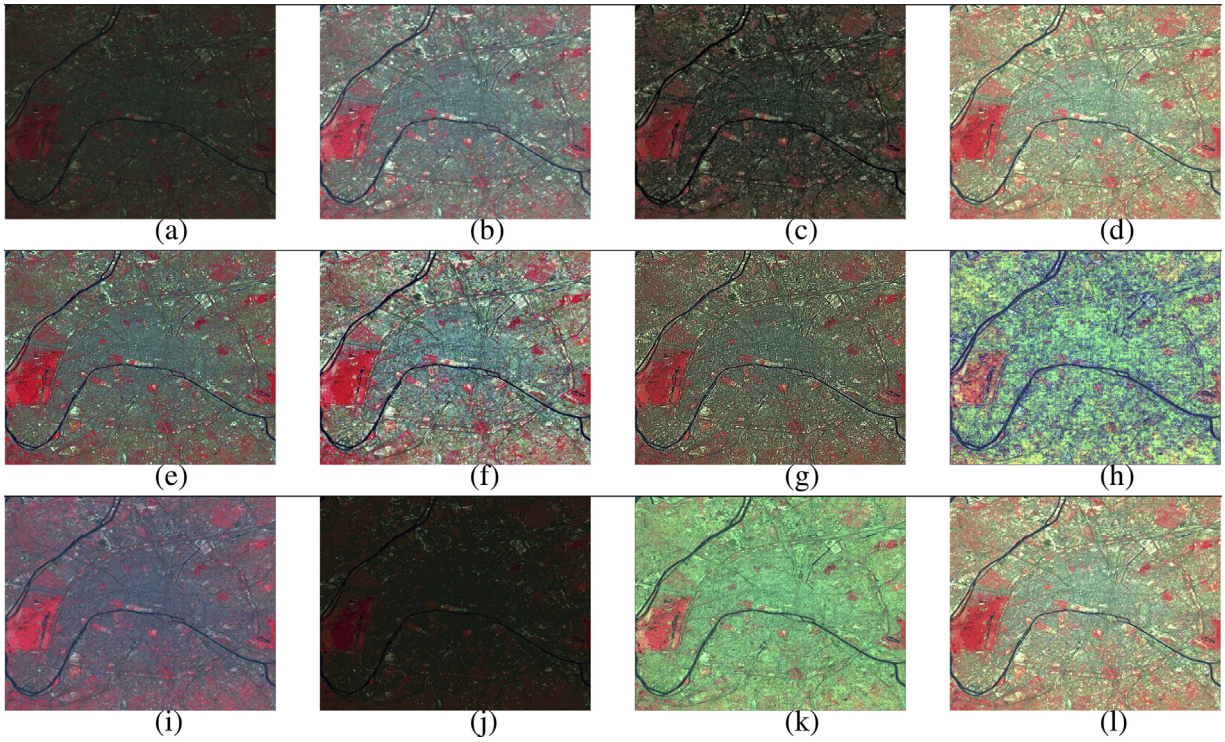

Fig. 8. Enhancement results of Image 5: (a) original, (b) DWT-SVD, (c) RHE-DCT, (d) LIME, (e) LCC, (f) TMM, (g) LSCN, (h) PSO, (i) DE-SA, (j) BDE, (k) PSO-CS and (l) proposed MDE.

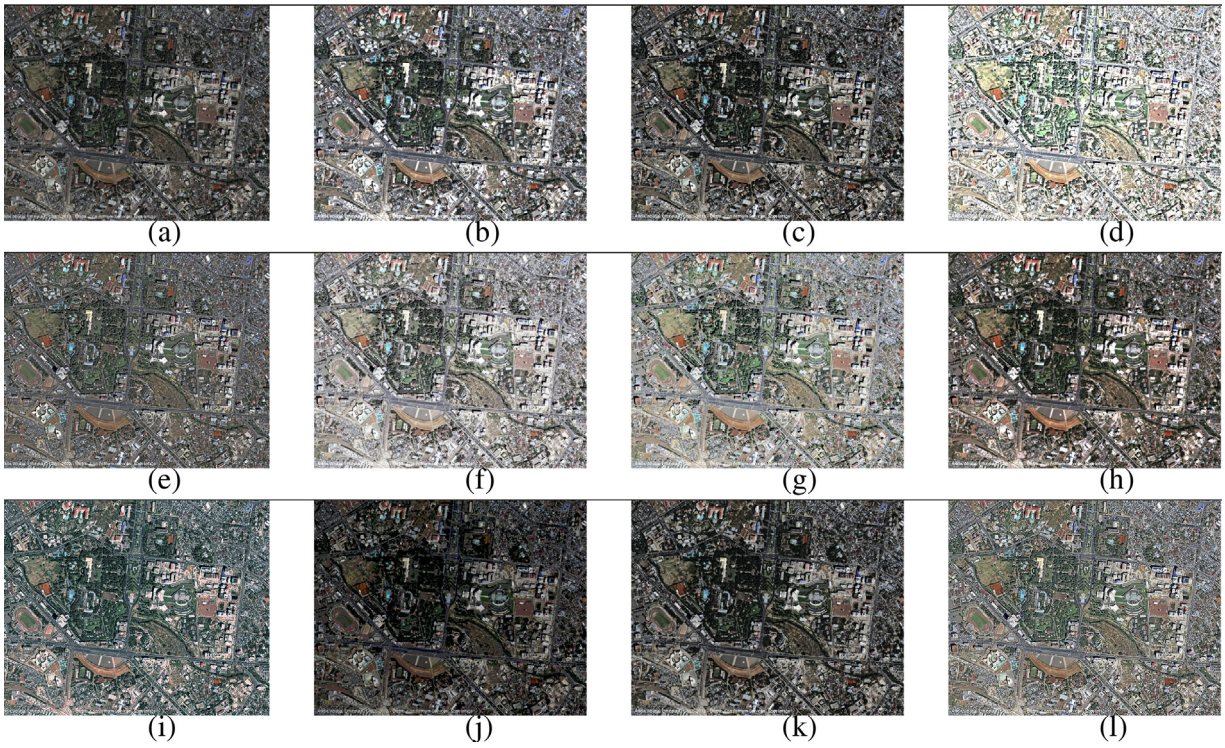

Fig. 9. Enhancement results of Image 6: (a) original, (b) DWT-SVD, (c) RHE-DCT, (d) LIME, (e) LCC, (f) TMM, (g) LSCN, (h) PSO, (i) DE-SA, (j) BDE, (k) PSO-CS and (l) proposed MDE.

to be same, they differ in the computational complexity of the random solution search phases, when analyzed separately. Even though, both the algorithms lacks in having a distinct exploration and exploitation phase, the total computational time required by both of them differs. The PSO algorithm is of more exploitive in nature, whereas DE is more exploratory. The exploration capability of DE is more fast and efficient and hence, it helps in quick convergence to the global optimum solutions compared with its PSO counterpart. Thus, a combination of DE with CS ensures a wise mixing of exploration and exploitation phases. Hence, instead of fixing

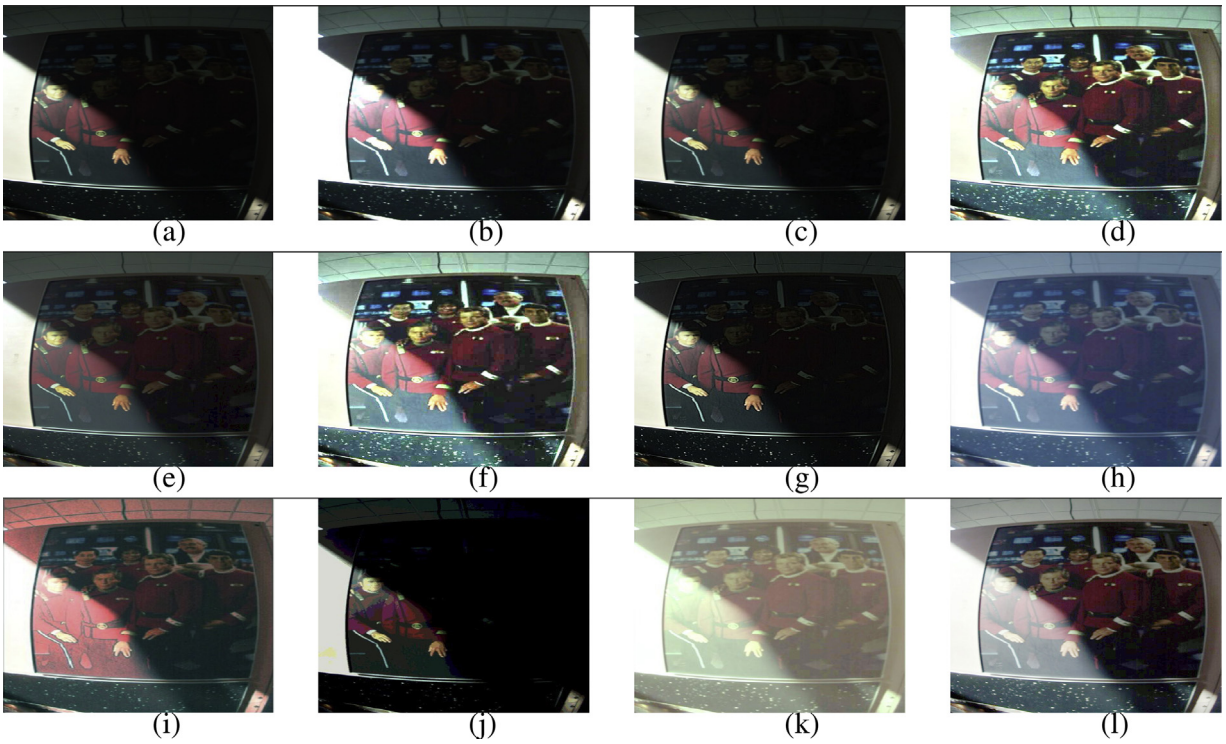

Fig. 10. Enhancement results of Image 7: (a) original, (b) DWT-SVD, (c) RHE-DCT, (d) LIME, (e) LCC, (f) TMM, (g) LSCN, (h) PSO, (i) DE-SA, (j) BDE, (k) PSO-CS and (l) proposed MDE.

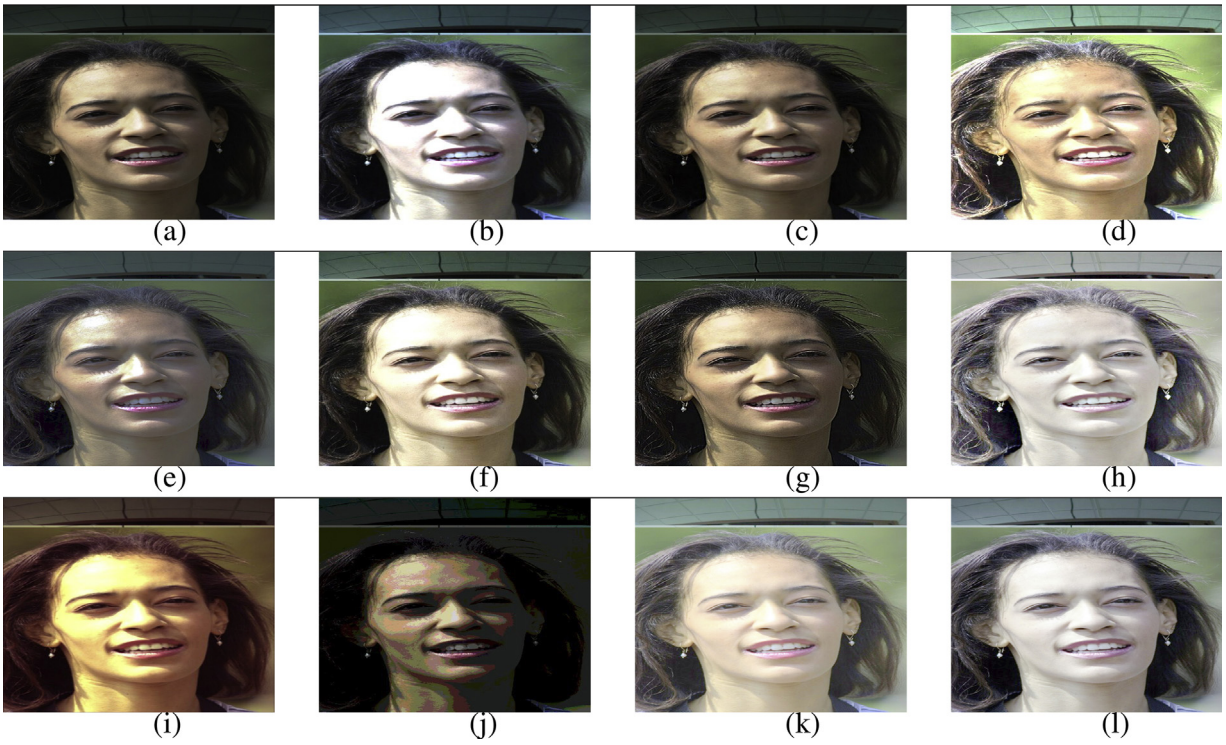

Fig. 11. Enhancement results of Image 8: (a) original, (b) DWT-SVD, (c) RHE-DCT, (d) LIME, (e) LCC, (f) TMM, (g) LSCN, (h) PSO, (i) DE-SA, (j) BDE, (k) PSO-CS and (l) proposed MDE.

each of these algorithms to run for a fixed number of iterations, a termination criterion can be devised based on an acceptable tolerance range for global fitness values attained in each run. This will evidently prove the computational efficiency of the proposed MDE algorithm in enhancing low contrast images.

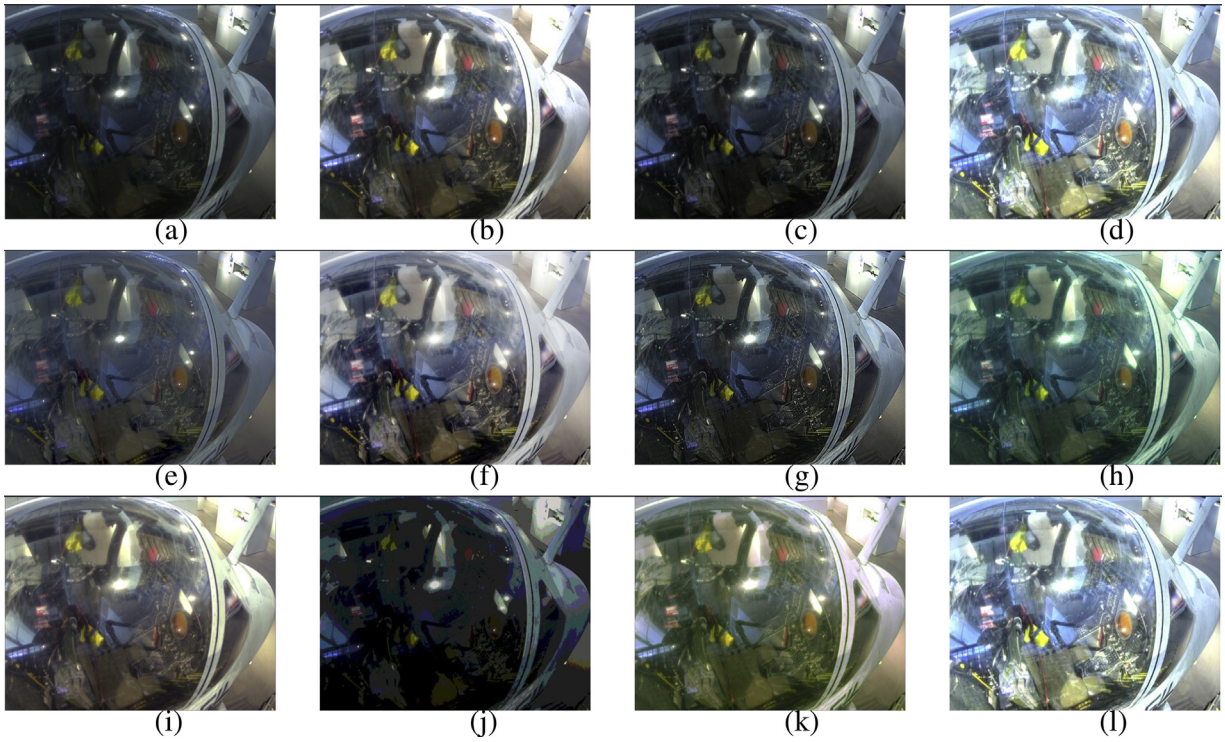

Fig. 12. Enhancement results of Image 9: (a) original, (b) DWT-SVD, (c) RHE-DCT, (d) LIME, (e) LCC, (f) TMM, (g) LSCN, (h) PSO, (i) DE-SA, (j) BDE, (k) PSO-CS and (l) proposed MDE.

Fig. 13. Enhancement results of Image 10: (a) original, (b) DWT-SVD, (c) RHE-DCT, (d) LIME, (e) LCC, (f) TMM, (g) LSCN, (h) PSO, (i) DE-SA, (j) BDE, (k) PSO-CS and (l) proposed MDE.

6. Conclusion

In this paper, a modified differential evolution (MDE) algorithm was proposed for enhancing the contrast and brightness of satellite images. The proposed optimization algorithm enhances the image by expanding its contrast depending on a defined transformation function. The iterative evaluation of the quality of enhanced image was done by validating it across a predefined fitness function. Local exploitation capability of CS algorithm driven by *Lévy* flight strategy is made use in the modified DE algorithm for improving its

performance. It ensured an increase in the convergence rate as compared with DE and CS algorithms by effectively avoiding its premature convergence, reaching the nearest approximation of the best possible solution. The proposed MDE algorithm evolved to be more stable and also helped in conserving the mean intensity of the image, bringing naturalness to the processed image. Quantitative and qualitative experimental studies were undertaken to demonstrate the robustness and efficiency of the proposed enhancement algorithm in comparison to other state-of-the-art techniques for different satellite and natural image datasets.

The proposed MDE algorithm has been tested on several satellite images and natural images in-order to substantiate its potency for enhancing images. The computed performance metrics revealed the superiority of the proposed algorithm over other state-of-the-art enhancement algorithms considered for brightness and contrast enhancement. Most of the algorithms developed over the past one decade, including histogram based and optimization based, were considered for comparison. Visual evaluation of enhancement results revealed the ability of the proposed algorithm to clearly distinguish the minor details present in the image without giving way to unwanted artifacts. The proposed algorithm also effectively conserves the mean intensity of the input image, preserving the naturalness of the scene captured. The proposed MDE algorithm was found well suited for enhancing not only satellite images, but also in improving the human perception of natural scenes.

On the other hand, the proposed MDE algorithm suffers a drawback of being computationally more complex. As a future step, the possibility of combining the favorable traits of other metaheuristics can also be explored. Such algorithms can also be extended to other related domains of image and signal processing to examine its usefulness.

Acknowledgements

The authors would like to thank the editor and anonymous reviewers for their valuable suggestions and comments which helped to improve the quality of the research paper.

References

[1] R.C. Gonzalez, R.E. Woods, Digital Image Processing, 2008, Nueva Jersey.
[2] S. Hashemi, S. Kiani, N. Noroozi, M.E. Moghaddam, An image contrast enhancement method based on genetic algorithm, Pattern Recognit. Lett. 31 (13) (2010) 1816–1824.
[3] Y.-T. Kim, Contrast enhancement using brightness preserving bi-histogram equalization, IEEE Trans. Consum. Electron. 43 (1) (1997) 1–8.
[4] Y. Wang, Q. Chen, B. Zhang, Image enhancement based on equal area dualistic sub-image histogram equalization method, IEEE Trans. Consum. Electron. 45 (1) (1999) 68–75.
[5] S.-D. Chen, A.R. Ramli, Contrast enhancement using recursive mean-separate histogram equalization for scalable brightness preservation, IEEE Trans. Consum. Electron. 49 (4) (2003) 1301–1309.
[6] C. Lee, C. Lee, C.-S. Kim, Contrast enhancement based on layered difference representation of 2D histograms, IEEE Trans. Image Process. 22 (12) (2013) 5372–5384.
[7] S.K. Pal, D. Bhandari, M.K. Kundu, Genetic algorithms for optimal image enhancement, Pattern Recognit. Lett. 15 (3) (1994) 261–271.
[8] F. Saitoh, Image contrast enhancement using genetic algorithm, in: Proceedings of the IEEE International Conference on Systems, Man, and Cybernetics, 1999, vol. 4, IEEE, 1999, pp. 899–904.
[9] C. Munteanu, V. Lazarescu, Evolutionary contrast stretching and detail enhancement of satellite images, in: Proceedings of MENDEL'99, 1999, pp. 94–99.
[10] C. Munteanu, A. Rosa, Towards automatic image enhancement using genetic algorithms, in: Proceedings of the Congress on Evolutionary Computation, 2000, vol. 2, IEEE, 2000, pp. 1535–1542.
[11] M. Braik, A.F. Sheta, A. Ayesh, Image enhancement using particle swarm optimization, in: World Congress on Engineering, vol. 1, 2007, pp. 978–988.
[12] A. Gorai, A. Ghosh, Gray-level image enhancement by particle swarm optimization, in: World Congress on Nature & Biologically Inspired Computing, NaBIC 2009, IEEE, 2009, pp. 72–77.
[13] A. Gorai, A. Ghosh, Hue-preserving color image enhancement using particle swarm optimization, in: 2011 IEEE Recent Advances in Intelligent Computational Systems (RAICS), IEEE, 2011, pp. 563–568.
[14] L. dos Santos Coelho, J.G. Sauer, M. Rudek, Differential evolution optimization combined with chaotic sequences for image contrast enhancement, Chaos Solitons Fractals 42 (1) (2009) 522–529.
[15] N.M. Kwok, Q.P. Ha, D. Liu, G. Fang, Contrast enhancement and intensity preservation for gray-level images using multiobjective particle swarm optimization, IEEE Trans. Autom. Sci. Eng. 6 (1) (2009) 145–155.
[16] P. Shanmugavadivu, K. Balasubramanian, Particle swarm optimized multi-objective histogram equalization for image enhancement, Opt. Laser Technol. 57 (2014) 243–251.
[17] Z. Ye, M. Wang, Z. Hu, W. Liu, An adaptive image enhancement technique by combining cuckoo search and particle swarm optimization algorithm, Comput. Intell. Neurosci. 2015 (2015) 13.
[18] A. Bhandari, A. Kumar, S. Chaudhary, G. Singh, A new beta differential evolution algorithm for edge preserved colored satellite image enhancement, Multidimens. Syst. Signal Process. (2015) 1–33.
[19] P. Hoseini, M.G. Shayesteh, Efficient contrast enhancement of images using hybrid ant colony optimisation genetic algorithm and simulated annealing, Digit. Signal Process. 23 (3) (2013) 879–893.
[20] A. Gogna, A. Tayal, Metaheuristics: review and application, J. Exp. Theor. Artif. Intell. 25 (4) (2013) 503–526.
[21] P.K. Mahapatra, S. Ganguli, A. Kumar, A hybrid particle swarm optimization and artificial immune system algorithm for image enhancement, Soft Comput. 19 (8) (2015) 2101–2109.
[22] A. Bhandari, V. Soni, A. Kumar, G. Singh, Cuckoo search algorithm based satellite image contrast and brightness enhancement using DWT-SVD, ISA Trans. 53 (4) (2014) 1286–1296.
[23] V. Singh, G. Kumar, G. Arora, Analytical evaluation for the enhancement of satellite images using swarm intelligence techniques, in: 3rd International Conference on Computing for Sustainable Global Development (INDIACom), IEEE, 2016, pp. 2401–2405.
[24] A.K. Jain, Fundamentals of Digital Image Processing, Prentice-Hall, Inc, 1989.
[25] S.M. Pizer, E.P. Amburn, J.D. Austin, R. Cromartie, A. Geselowitz, T. Greer, B. ter Haar Romeny, J.B. Zimmerman, K. Zuiderveld, Adaptive histogram equalization and its variations, Comput. Vis. Graph. Image Process. 39 (3) (1987) 355–368.
[26] J.A. Stark, Adaptive image contrast enhancement using generalizations of histogram equalization, IEEE Trans. Image Process. 9 (5) (2000) 889–896.
[27] S. Gupta, Y. Kaur, Review of different local and global contrast enhancement techniques for a digital image, Int. J. Comput. Appl. 100 (18) (2014) 18–23.
[28] X. Zhou, Q. Shen, J. Wang, Research of image enhancement based on particle swarm optimization, Microelectron. Comput. 25 (4) (2008) 42–44.
[29] R. Jain, R. Kasturi, B.G. Schunck, Machine Vision, vol. 5, McGraw-Hill, New York, 1995.
[30] J. Canny, A computational approach to edge detection, IEEE Trans. Pattern Anal. Mach. Intell. 6 (1986) 679–698.
[31] P. Sarangi, B. Mishra, B. Majhi, S. Dehuri, Gray-level image enhancement using differential evolution optimization algorithm, in: International Conference on Signal Processing and Integrated Networks (SPIN), 2014, IEEE, 2014, pp. 95–100.
[32] R. Storn, K. Price, Differential evolution-a simple and efficient heuristic for global optimization over continuous spaces, J. Glob. Optim. 11 (4) (1997) 341–359.
[33] K. Price, R.M. Storn, J.A. Lampinen, Differential Evolution: A Practical Approach to Global Optimization, Springer Science & Business Media, 2006.
[34] X.-S. Yang, Nature-Inspired Optimization Algorithms, Elsevier, 2014.
[35] X.-S. Yang, S. Deb, Cuckoo search via Lévy flights, in: World Congress on Nature & Biologically Inspired Computing, NaBIC 2009, IEEE, 2009, pp. 210–214.
[36] F. Xue, A.C. Sanderson, R.J. Graves, Multi-objective differential evolution – algorithm, convergence analysis, and applications, in: 2005 IEEE Congress on Evolutionary Computation, vol. 1, IEEE, 2005, pp. 743–750.
[37] D. Zaharie, Influence of crossover on the behavior of differential evolution algorithms, Appl. Soft Comput. 9 (3) (2009) 1126–1138.
[38] S. Das, P.N. Suganthan, Differential evolution: a survey of the state-of-the-art, IEEE Trans. Evol. Comput. 15 (1) (2011) 4–31.
[39] G. Jeyakumar, C. Shanmugavelayutham, Convergence Analysis of Differential Evolution Variants on Unconstrained Global Optimization Functions, Int. J. Artif. Intell. Appl. 2 (2) (2011) 116–127 arXiv:1105.1901.
[40] D. Zaharie, Differential evolution from theoretical analysis to practical insights, in: Proceeding of 19th International Conference on Soft Computing, Brno, Czech Republic, 2013, pp. 26–28.
[41] N.E. Humphries, N. Queiroz, J.R. Dyer, N.G. Pade, M.K. Musyl, K.M. Schaefer, D.W. Fuller, J.M. Brunnschweiler, T.K. Doyle, J.D. Houghton, et al., Environmental context explains Lévy and Brownian movement patterns of marine predators, Nature 465 (7301) (2010) 1066–1069.
[42] X.-S. Yang, T. Ting, M. Karamanoglu, Random walks Lévy flights Markov chains and metaheuristic optimization, in: Future Information Communication Technology and Applications, Springer, 2013, pp. 1055–1064.
[43] S. Suresh, S. Lal, An efficient cuckoo search algorithm based multilevel thresholding for segmentation of satellite images using different objective functions, Expert Syst. Appl. 58 (2016) 184–209.
[44] M. Leccardi, Comparison of three algorithms for Levy noise generation, in: Proceedings of Fifth EUROMECH Nonlinear Dynamics Conference, 2005.

[45] A.S.P. Joko Siswantoro, Soft Computing Applications and Intelligent Systems, Springer, 2013.
[46] H. Demirel, C. Ozcinar, G. Anbarjafari, Satellite image contrast enhancement using discrete wavelet transform and singular value decomposition, IEEE Geosci. Remote Sens. Lett. 7 (2) (2010) 333–337.
[47] X. Fu, J. Wang, D. Zeng, Y. Huang, X. Ding, Remote sensing image enhancement using regularized-histogram equalization and DCT, IEEE Geosci. Remote Sens. Lett. 12 (11) (2015) 2301–2305.
[48] J.-L. Lisani, J. Michel, J.-M. Morel, A.B. Petro, C. Sbert, An inquiry on contrast enhancement methods for satellite images, IEEE Trans. Geosci. Remote Sens. 54 (12) (2016) 7044–7054.
[49] A. Moore, J. Allman, R.M. Goodman, A real-time neural system for color constancy, IEEE Trans. Neural Netw. 2 (2) (1991) 237–247.
[50] Z. Mai, H. Mansour, R. Mantiuk, P. Nasiopoulos, R. Ward, W. Heidrich, Optimizing a tone curve for backward-compatible high dynamic range image and video compression, IEEE Trans. Image Process. 20 (6) (2011) 1558–1571.
[51] X. Guo, LIME: A Method for Low-light IMage Enhancement, In Proceedings of the 2016 ACM on Multimedia Conference 2016 (2016) 87–91 arXiv:1605.05034.
[52] K. Zhan, J. Shi, J. Teng, Q. Li, M. Wang, F. Lu, Linking synaptic computation for image enhancement, Neurocomputing 238 (2017) 1–12.
[53] A. Gogna, A. Tayal, Comparison of hybrid and classical metaheuristic for automatic image enhancement, Int. J. Comput. Appl. (2012) 0975–8887.
[54] Q. Huynh-Thu, M. Ghanbari, Scope of validity of PSNR in image/video quality assessment, Electron. Lett. 44 (13) (2008) 800–801.
[55] Z. Wang, A.C. Bovik, A universal image quality index, IEEE Signal Process. Lett. 9 (3) (2002) 81–84.
[56] L. Zhang, L. Zhang, X. Mou, D. Zhang, FSIM: a feature similarity index for image quality assessment, IEEE Trans. Image Process. 20 (8) (2011) 2378–2386.
[57] A. Bhandari, A. Kumar, G. Singh, V. Soni, Dark satellite image enhancement using knee transfer function and gamma correction based on DWT-SVD, Multidimens. Syst. Signal Process. 27 (2) (2016) 453–476.
[58] C.P. Loizou, C.S. Pattichis, M. Pantziaris, T. Tyllis, A. Nicolaides, Quality evaluation of ultrasound imaging in the carotid artery based on normalization and speckle reduction filtering, Med. Biol. Eng. Comput. 44 (5) (2006) 414–426.
[59] S.H. Bae, M. Kim, A novel image quality assessment with globally and locally consilient visual quality perception, IEEE Trans. Image Process. 25 (5) (2016) 2392–2406.
[60] S.H. Bae, M. Kim, A novel DCT-based JND model for luminance adaptation effect in DCT frequency, IEEE Signal Process. Lett. 20 (9) (2013) 893–896.
[61] C.E. Shannon, A mathematical theory of communication, Bell Syst. Tech. J. 27 (4) (1948) 623–656.
[62] Y. Fang, K. Ma, Z. Wang, W. Lin, Z. Fang, G. Zhai, No-reference quality assessment of contrast-distorted images based on natural scene statistics, IEEE Signal Process. Lett. 22 (7) (2015) 838–842.
[63] A.A. Michelson, Studies in Optics, Courier Corporation, 1995.
[64] S.E. Susstrunk, S. Winkler, Color image quality on the internet, in: Electronic Imaging 2004, International Society for Optics and Photonics, 2003, pp. 118–131.
[65] M. Frackiewicz, H. Palus, New image quality metric used for the assessment of color quantization algorithms, in: Ninth International Conference on Machine Vision, International Society for Optics and Photonics, 2017, pp. 103411G.